

Cisplatin enhances PERK- and CD95-dependent MDA-7/IL-24-induced killing in ovarian carcinoma cells

**Adly Yacoub, Renyan Liu, Margaret A. Park, Hossein A. Hamed, Rupesh Dash, Danielle N. Schramm,
Devanand Sarkar, Igor P. Dimitriev, Jessica K. Bell, Steven Grant, Nicholas P. Farrell,
David T. Curiel, Paul B. Fisher and Paul Dent***

Departments of Biochemistry and Molecular Biology (AY, RL, MAP, DNS, JKB, HAH, SG, PD), Medicine (SG), Human and Molecular Genetics (RD, DS, PBF), VCU Institute for Molecular Medicine (DS, SG, PBF, PD), VCU Massey Cancer Center (DS, SG, PBF, PD), Department of Chemistry (NPF), Virginia Commonwealth University, School of Medicine, 401 College St., Richmond, VA 23298; Division of Human Gene Therapy (IPD, DTC), Departments of Medicine, Pathology and Surgery, and the Gene Therapy Center, University of Alabama at Birmingham, Birmingham, AL 35294.

Running Title: MDA-7/IL-24 and cisplatin

Abbreviations: ERK: extracellular regulated kinase; MEK: mitogen activated extracellular regulated kinase; JNK: c-Jun NH₂-terminal kinase; PI3K: phosphatidyl inositol 3 kinase; MDA-7/IL-24: melanoma differentiation associated gene-7/Interleukin-24; PERK: protein kinase R –like endoplasmic reticulum kinase. MAPK: mitogen activated protein kinase; ca: constitutively active; dn: dominant negative; EGFR: epidermal growth factor receptor; IL: interleukin; PTEN: phosphatase and tensin homologue on chromosome ten.

*Correspondence to:

Paul Dent

401 College Street

Massey Cancer Center, Box 980035

Department of Biochemistry and Molecular Biology

Virginia Commonwealth University

Richmond VA 23298-0035.

Tel: 804 628 0861

Fax: 804 827 1309

pdent@vcu.edu

Number of text pages: 30

Number of Tables: 0

Number of Figures: 5

Words in Abstract: 250

Words in Introduction: 986

Words in Discussion: 1,506

Abstract

Melanoma differentiation associated gene-7/interleukin 24 (*mda-7/IL-24*) is a unique IL-10 family cytokine displaying selective apoptosis-inducing activity in transformed cells without harming normal cells. The present studies focused on defining the mechanism(s) by which recombinant adenoviral delivery of MDA-7/IL-24 inhibits cell survival of human ovarian carcinoma cells (OCC). Expression of MDA-7/IL-24 induced phosphorylation of protein kinase R-like endoplasmic reticulum kinase (PERK) and eIF2 α . In a PERK-dependent fashion MDA-7/IL-24 reduced ERK1/2 and AKT phosphorylation and activated JNK1/2 and p38 MAPK. MDA-7/IL-24 reduced MCL-1 and BCL-XL and increased BAX levels via PERK signaling; cell killing was mediated via the intrinsic pathway and cell killing was primarily necrotic as judged using Annexin V–PI staining. Inhibition of p38 MAPK and JNK1/2 abolished MDA-7/IL-24 toxicity and blocked BAX and BAK activation, whereas activation of MEK1/2 or AKT suppressed enhanced killing and JNK1/2 activation. MEK1/2 signaling increased expression of the MDA-7/IL-24 and PERK chaperone BiP/GRP78, and over-expression of BiP/GRP78 suppressed MDA-7/IL-24 toxicity. MDA-7/IL-24-induced LC3-GFP vesicularization and processing of LC3; and knockdown of ATG5 suppressed MDA-7/IL-24-mediated toxicity. MDA-7/IL-24 and cisplatin interacted in a greater than additive fashion to kill tumor cells that was dependent upon a further elevation of JNK1/2 activity and recruitment of the extrinsic CD95 pathway. MDA-7/IL-24 toxicity was enhanced in a weak additive fashion by paclitaxel; paclitaxel enhanced MDA-7/IL-24 + cisplatin lethality in a greater than additive fashion via BAX. Collectively, our data demonstrate that MDA-7/IL-24 induces an ER stress response that activates multiple pro-apoptotic pathways culminating in decreased ovarian tumor cell survival.

Introduction

In the United States, ovarian carcinoma (OC) is diagnosed in ~26,000 patients per annum with ~15,000 deaths. If the disease is detected at a very early stage, in which a large portion or the entire ovary can be removed with the tumor, ~75% of patients survive at least 5-years post-diagnosis (Coleman and Sood, 2006,). However, in the majority of cases, if the disease has spread beyond the ovary into the peritoneum with nodal involvement, even under ideal circumstances where the disease is still only locally advanced, and in which essentially all of the tumor can be surgically removed and the patients are maximally treated with chemotherapies including cisplatin and Taxanes, the prognosis is poor with rapid nadir.

The *mda-7/IL-24* gene was isolated from human melanoma cells treated with interferon and mezerein (Jiang et al, 1995; Staudt et al, 2009). The expression of MDA-7/IL-24 is decreased in advanced melanomas, with undetectable levels in metastatic disease (Jiang et al, 1995; Ekmekcioglu et al., 2001; Ellerhorst et al, 2002; Huang et al, 2001; Parrish-Novak et al, 2002; Caudell et al, 2002; Pestka et al, 2004; Gupta et al, 2006; Lebedeva et al, 2005; Fisher et al, 2003; Fisher, 2005; Fisher et al, 2007). Enforced expression of MDA-7/IL-24 inhibits the growth and kills a broad spectrum of cancer cells, without exerting deleterious effects in normal human epithelial or fibroblast cells (Gupta et al, 2006; Lebedeva et al, 2005; Fisher et al, 2003; Fisher et al, 2007; Su et al, 2001; Su et al, 1998). Considering its potent cancer-specific apoptosis-inducing ability and tumor growth-suppressing properties in human tumor xenograft animal models, *mda-7/IL-24* was evaluated in a phase I clinical trial in patients with advanced cancers, including melanomas (Lebedeva et al, 2005; Fisher et al, 2003; Fisher et al, 2007; Cunningham et al, 2005; Emdad et al, 2009). This study indicated that Ad.*mda-7* injected intra-tumorally was safe and with repeated injection, significant clinical activity was evident in patients that had not responded to a spectrum of other therapies, including radiation, chemotherapy and immunotherapy, applied alone or in various combinations.

The apoptotic pathways by which *Ad.mda-7* causes cell death are not fully understood, however, current evidence suggests an inherent complexity and an involvement of proteins important for the onset of growth inhibition and apoptosis (Gupta et al, 2006; Lebedeva et al, 2005; Fisher et al, 2003; Fisher et al, 2005; Su et al, 2001; Su et al, 1998; Emdad et al, 2009). In melanoma cell lines, but not in normal melanocytes, *Ad.mda-7* infection induces a significant decrease in both BCL-2 and BCL-XL levels, with only a modest up-regulation of BAX and BAK expression (Lebedeva et al, 2002; Gupta et al, 2006; Lebedeva et al, 2005; Fisher et al, 2003; Fisher et al, 2005; Su et al, 2001; Su et al, 1998; Lebedeva et al, 2002). The ability of *Ad.mda-7* to induce apoptosis in DU-145 prostate cancer cells, which does not produce BAX, indicates that MDA-7/IL-24 can also mediate apoptosis in tumor cells by a BAX-independent pathway (Lebedeva et al, 2003; Su et al, 2006). In prostate cancer cells, over-expression of either BCL-2 or BCL-XL protects cells from *Ad.mda-7*-induced toxicity in a cell type-dependent fashion (Lebedeva et al, 2003; Su et al, 2006). The combination of radiation and *mda-7/IL-24* enhances lethality in ovarian cancer cells (OCC) (Emdad et al, 2006). In one OCC line, MDA-7/IL24 was reported to kill via the extrinsic apoptosis pathway (Gopalan et al, 2005). Thus, MDA-7/IL-24 lethality seems to occur by multiple distinct pathways in different cell types but in all of these studies, cell killing is reflected in a profound induction of mitochondrial dysfunction.

MDA-7/IL-24 toxicity has been linked to alterations in endoplasmic reticulum (ER) stress signaling (Gupta et al, 2006a; Gupta et al, 2006b). In these studies, MDA-7/IL-24 physically associates with BiP/GRP78 and inactivates the protective actions of this ER-chaperone protein. In addition to virus-administered *mda-7/IL-24*, delivery of this cytokine as a bacterially expressed glutathione-S-transferase (GST) fusion protein, GST-MDA-7, retains cancer specific killing, selective ER localization and induces similar signal transduction changes in cancer cells (Sauane et al, 2004). High concentrations of GST-MDA-7 or infection with *Ad.mda-7* kill human glioma cells and do so in a PERK-dependent fashion that is dependent on mitochondrial dysfunction (Yacoub et al, 2004; Yacoub et al, 2008; Yacoub et al, 2008a; Yacoub et al, 2008b). The precise mechanisms by which GST-MDA-7 or *Ad.mda-7* modulates survival in human OCC are unknown.

Our laboratories have demonstrated that Ad.*mda-7* kills melanoma cells in part by promoting p38 MAPK-dependent activation of the growth arrest and DNA damage inducible genes, including GADD153, GADD45 and GADD34 (Sarkar et al, 2002; Yacoub et al, 2003; Sarkar et al, 2002; Mhashilkar et al, 2003; Chada et al, 2005; Sauane et al, 2004). In primary glioblastoma (GBM) cells we noted p38 MAPK signaling as a protective signal (Yacoub et al, 2008b). Other groups have argued that inhibition of PI3K signaling, but not ERK1/2 signaling, modestly promotes Ad.*mda-7* lethality in breast and lung cancer cells (Mhashilkar et al, 2003; Chada et al, 2005). GST-MDA-7 protein, in the 0.25-2.0 nM concentration range causes growth arrest with little cell killing, whereas at ~20-fold greater concentrations, this cytokine causes profound growth arrest and tumor cell death (Yacoub et al, 2008a; Yacoub et al, 2008b; Sauane et al, 2004). Utilizing established human OCC lines we presently examined the impact of GST-MDA-7 and Ad.*mda-7* on viability with a focus on elucidating the molecular mechanisms by which MDA-7/IL-24 enhances tumor cell death.

Materials and Methods.

Materials.

SKOVIII and OVCAR OCC were purchased from the ATCC. Caspase inhibitors and Taxol were supplied by Calbiochem (San Diego, CA) as powder, dissolved in sterile DMSO, and stored frozen under light-protected conditions at -80°C . Plasmids expressing dominant negative PERK, BiP/GRP78 and LC3-GFP were kindly supplied by Drs. A. Diehl (University of Pennsylvania), A. Lee (UCLA), and S. Spiegel (VCU). Short hairpin RNA constructs targeting *ATG5* (pLVTHM/*ATG5*), were a generous gift from Dr. Yousefi, Department of Pharmacology, University of Bern, Bern Switzerland. Commercially available validated short hairpin RNA molecules to knockdown RNA/protein levels were from Qiagen (Valencia, CA): *ATG5* (SI02655310). Cisplatin was purchased from Sigma (St. Louis, MO). Antibody reagents, kinase inhibitors, caspase inhibitors cell culture reagents, and non-commercial recombinant adenoviruses have been previously described by ourselves and others (Yacoub et al, 2008a; Yacoub et al, 2008b; Sarkar et al, 2002; Guicciardi et al, 2000; Park et al, 2008; Park et al, 2009; Zhang et al, 2008). The Annexin V / PI kit was from (BD PharMingen).

Methods.

Generation of Ad.5-mda-7 or Ad.5/3-mda-7 and synthesis of GST-MDA-7. Recombinant type 5 and 5/3 adenoviruses to express MDA-7/IL-24 (*Ad.mda-7*), or control (CMV vector) were generated using recombination in HEK293 cells as described in (Yacoub et al, 2008; Sarkar et al, 2002). *Ad.5/3-mda-7* was prepared as previously described (Dash et al, 2009).

Cell culture and in vitro exposure of cells to GST-MDA-7 and drugs. All established OCC lines were cultured at 37°C (5% (v/v) CO_2) *in vitro* using RPMI supplemented with 5% (v/v) fetal calf serum and 10% (v/v) Non-essential amino acids. For short-term cell killing assays and immunoblotting, cells were plated at a density of 3×10^3 per cm^2 and 36 h after plating were treated with MDA-7/IL-24 and/or various drugs, as indicated. *In vitro* small molecule inhibitor treatments were from a 100 mM stock solution of each drug and the maximal concentration of Vehicle (DMSO) in media was 0.02% (v/v). For adenoviral infection, cells

were infected 12 h after plating and the expression of the recombinant viral transgene allowed to occur for 24 h prior to any additional experimental procedure. Cells were not cultured in reduced serum media during any study.

Cell treatments, SDS-PAGE and Western blot analysis. Cells were treated with various GST-MDA-7 concentrations or viral multiplicities of infection, as indicated in the Figure legends. For SDS PAGE and immunoblotting, cells were lysed in either a non-denaturing lysis buffer, and prepared for immunoprecipitation as described in (Yacoub et al, 2008a; Park et al, 2009) or in whole-cell lysis buffer (0.5 M Tris-HCl, pH 6.8, 2% SDS, 10% glycerol, 1% β -mercaptoethanol, 0.02% bromophenol blue), and the samples were boiled for 30 min. After immunoprecipitation, samples were boiled in whole cell lysis buffer. The boiled samples were loaded onto 10-14% SDS-PAGE and electrophoresis was run overnight. Proteins were electrophoretically transferred onto 0.22 μ m nitrocellulose, and immunoblotted with indicated primary antibodies against the different proteins.

Recombinant adenoviral vectors; infection in vitro. We generated or purchased previously noted recombinant adenoviruses to express constitutively activated and dominant negative AKT and MEK1 proteins, dominant negative caspase 9, XIAP, c-FLIP-s, CRM A, and BCL-XL (Vector Biolabs, Philadelphia, PA). Cells were infected with these adenoviruses at an approximate m.o.i. of 50. Cells were incubated for 24h to ensure adequate expression of transduced gene products prior to drug exposures.

Detection of cell death by Trypan Blue, Hoechst, TUNEL and flow cytometric assays. Cells were harvested by trypsinization with Trypsin/EDTA for ~10 min at 37°C. As some apoptotic cells detached from the culture substratum into the medium, these cells were also collected by centrifugation of the medium at 1,500 rpm for 5 min. The pooled cell pellets were resuspended and mixed with trypan blue dye. Trypan blue stain, in which blue dye incorporating cells were scored as being dead was performed by counting of cells using a light

microscope and a hemacytometer. Five hundred cells from randomly chosen fields were counted and the number of dead cells was counted and expressed as a percentage of the total number of cells counted. For confirmatory purposes the extent of apoptosis was evaluated by assessing Hoechst and TUNEL stained cytospin slides under fluorescent light microscopy and scoring the number of cells exhibiting the “classic” morphological features of apoptosis and necrosis. For each condition, 10 randomly selected fields per slide were evaluated, encompassing at least 1500 cells. Alternatively, the Annexin V/propidium iodide assay was carried out to determine cell viability as per the manufacturer's instructions (BD PharMingen) using a Becton Dickinson FACScan flow cytometer (Mansfield, MA).

Colony Formation Assay. Single cells were plated (250-1500 cells) per 60 mm dish. Twelve h after plating cells were infected with Ad.5-*cmv* or Ad.5-*mda-7* at 80 m.o.i. and 24h after infection cells were treated with vehicle or cisplatin (CDDP, 3 μ M). The media was changed to drug free media 48 h after CDDP treatment and colonies of > 50 cells / colony permitted to form for 10-14 days.

Plasmid transfection. Plasmid DNA (0.5 μ g / total plasmid transfected) was diluted into 50 μ l of RPMI growth media that lacked supplementation with FBS or with penicillin-streptomycin. Lipofectamine 2000 reagent (1 μ l) (Invitrogen, Carlsbad, CA) was diluted into 50 μ l growth media that lacked supplementation with FBS or with penicillin-streptomycin. The two solutions were then mixed together and incubated at room temperature for 30 min. The total mix was added to each well (4-well glass slide or 12-well plate) containing 200 μ l growth media that lacked supplementation with FBS or with penicillin-streptomycin. The cells were incubated for 4 h at 37°C, after which the media was replaced with RPMI growth media containing 5% (v/v) FBS and 1x pen-strep.

Microscopy for LC3-GFP expression. Where indicated LC3-GFP transfected cells, 12h after transfection were infected with either Ad.5-*cmv* or Ad.5-*mda-7* and then cultured for 24 h. Cells were then stained with LysoTracker Red Dye (Invitrogen) at the indicated time points for 20 min. LysoTracker Red Dye stained cells

were visualized immediately after staining on a Zeiss Axiovert 200 microscope using the rhodamine filter.

LC3-GFP transfected cells were visualized at the indicated time points on the Zeiss Axiovert 200 microscope using the FITC filter.

Data analysis. Comparison of the effects of various treatments was performed using one way analysis of variance and a two tailed Student's *t*-test. Differences with a *p*-value of < 0.05 were considered statistically significant. Experiments shown are the means of multiple individual points from multiple experiments (\pm SEM).

Results

Initial experiments focused on defining the dose-dependent impact of GST-MDA-7 on OCC growth and viability. GST-MDA-7 in a dose-dependent manner suppressed the proliferation of SKOVIII and OVCAR cells (Figure 1A and 1B), with a reduced effect in SKOVIII. These findings correlated with dose-dependent cell killing by GST-MDA-7 in these cells; of note, GST-MDA-7 suppressed tumor cell proliferation without causing a large degree of cell death in both OCC (Figure 1B; *cf* Figure 1A). In a similar manner as observed with GST-MDA-7 protein, increasing multiplicities of infection of a type 5 recombinant adenovirus expressing MDA-7/IL-24, Ad.5-*mda-7*, resulted in dose-dependent tumor cell killing (Figure 1C). In contrast to several prior studies in other tumor cell types we noted in OCC that infection with a recombinant adenovirus to express MDA-7/IL-24 was at least as efficacious at killing cells as was treatment with GST-MDA-7. As a result of this observation, we focused our studies using Ad.5-*mda-7*.

Infection of OCC (OVCAR) with Ad.5-*mda-7* promoted cleavage of caspase 3 and PARP1 processing of LC3 within 48h (Figure 2A). Similar data were obtained in SKOVIII cells (Figure S1). Expression of MDA-7/IL-24 induced phosphorylation of protein kinase R–like endoplasmic reticulum kinase (PERK) and eIF2 α . In a PERK-dependent fashion MDA-7/IL-24 also reduced ERK1/2 and AKT phosphorylation and activated JNK1/2 and p38 MAPK (Figure 2B). MDA-7/IL-24 lowered expression of MCL-1 and BCL-XL and increased BAX levels via PERK signaling. Inhibition of both p38 MAPK and JNK1/2 signaling blocked Ad.5-*mda-7* lethality that correlated with reduced activation of BAX and BAK (Figures 2C and 2D). Sustained activation of AKT or of MEK1 using molecular tools suppressed Ad.5-*mda-7* toxicity (Figure 2E). Additional suppression of AKT or MEK1 function using dominant negative constructs further enhanced MDA-7/IL-24 lethality. In SKOVIII cells, that were more resistant to MDA-7/IL-24 lethality than OVCAR cells, we noted that inhibition of the extrinsic pathway using c-FLIP-s or CRM A expression blunted MDA-7/IL-24–induced killing whereas in OVCAR cells neither c-FLIP-s nor CRM A impacted on MDA-7/IL-24 toxicity (Figure 2E).

Prior studies by our laboratories have demonstrated that MDA-7/IL-24–induced activation of PERK was a toxic signal that promoted activation of the JNK pathway as well as a toxic form of autophagy (Yacoub et al, 2008b). In OVCAR cells, Ad.5-*mda-7* infection promoted a PERK-dependent vesicularization of a transfected LC3-GFP construct; vesicularization was blocked by knockdown of *ATG5* expression (data not shown). Expression of dominant negative PERK, BiP/GRP78 or knock down of *ATG5* suppressed Ad.*mda-7* lethality (Figure 2F).

Prior studies from our laboratories, including those in Figures 1 and 2, have used recombinant type 5 adenoviruses to deliver MDA-7/IL24 to brain cancer cells (Ad.5-*mda-7*) (e.g., Yacoub et al., 2008). Some OCC tumor cell lines, and other tumor cell types such as renal carcinoma and malignant GBM cells, are in general not readily amenable to gene therapy approaches using low particle levels of type 5 adenovirus due to their reduced expression of Coxsackie and adenovirus receptor (CAR) (Park et al, 2009). Because of this, we generated a recombinant adenovirus to express MDA-7/IL24, which contained a modified serotype viral knob from type 5 and from type 3 adenoviruses (Ad.5/3-*mda-7*) (Dash et al, 2009). OCC were poorly killed following exposure to an Ad.5-*mda-7* infection at a multiplicity of infection of 20 particles per cell (Figure 3A). Infection of OCC using an Ad.5/3-*mda-7* virus caused significant amounts of cell killing at either 20 or 80 m.o.i. (Figure 3A). This data argues that modified serotype type 5 / serotype 3 recombinant viruses may represent useful gene delivery system in ovarian carcinoma.

Platinum containing chemotherapeutic drugs are a well established modality for the treatment of ovarian cancer. Infection of tumor cells with Ad.5-*mda-7* enhanced the toxicity of cisplatin (Figure 3B). Similar data to that in OCC using cisplatin was also observed in primary human GBM cells (Figure S2). Enhanced toxicity of cisplatin when combined with an oncolytic adenovirus expressing MDA-7/IL-24 has also been observed in hepatocellular carcinoma cells (Wu et al, 2009). BBR3464 is a novel platinum-based drug that has undergone phase II evaluation. In a similar manner to cisplatin, infection of tumor cells with Ad.5-*mda-7* enhanced the toxicity of BBR3464 (Figure 3C). Similar data to that in OCC using BBR3464 was also

observed in primary human GBM cells (Figure S3). In colony formation assays, Ad.5-*mda-7* and cisplatin interacted in a greater than additive fashion to suppress clonogenic survival (Figure 3D).

We next determined the impact of Ad.5-*mda-7* infection and cisplatin treatment on the activities of survival-signaling kinases and apoptosis regulatory caspases. Expression of MDA-7/IL-24 promoted cleavage of caspase 3, and activation of JNK1/2, p38 MAPK and PERK (Figure 4A). Treatment of cells expressing MDA-7/IL-24 with cisplatin caused additional cleavage of caspase 3, and activation of JNK1/2, but not additional activation of PERK. Expression of activated MEK1 EE increased the protein levels of BiP/GRP78 and blocked MDA-7/IL-24-induced activation of PERK. These effects correlated with sustained activation of ERK1/2 and reduced activation of JNK1/2 and of caspase 3. Expression of dominant negative MEK1 suppressed ERK1/2 activity and BiP/GRP78 levels, and enhanced MDA-7/IL-24-induced JNK1/2 and PERK activation and cleavage of caspase 3. Co-expression of dominant negative MEK1 and dominant negative AKT significantly enhanced the toxicities of MDA-7/IL-24, cisplatin and MDA-7/IL-24 + cisplatin treatments (Figure 4B). Expression of constitutively activated forms of either MEK1 or AKT suppressed MDA-7/IL-24 + cisplatin toxicity. Inhibition of caspase 9 or JNK pathway signaling blocked MDA-7/IL-24 + cisplatin-induced killing (Figure 4C). Over-expression of BiP/GRP78 also suppressed MDA-7/IL-24 and MDA-7/IL-24 + cisplatin-induced killing as measured in trypan blue dye exclusion assays, which correlated with reduced activation of PERK and sustained expression of MCL-1 and c-FLIP-s (Figure 4C, inset panel). Very similar data to those using trypan blue were obtained using Annexin V-PI flow cytometry analyses (Figure 4D).

In contrast to the minimal effects on altering MDA-7/IL-24 lethality as a single agent, inhibition of caspase 8 function expressing either c-FLIP-s or CRM A prevented cisplatin enhancing MDA-7/IL-24-induced killing (Figure 4E). Prior studies in renal cancer cells have shown that ceramide synthase 6 plays a key role in MDA-7/IL-24 lethality, implicating the *de novo* ceramide synthesis pathway as a mediator of MDA-7/IL-24 effects (Park et al., 2009). Knock down of ceramide synthase 6 expression suppressed MDA-7/IL-24 and

MDA-7/IL-24 + cisplatin lethality (Figure 4E). Knockdown of ATG5 also suppressed MDA-7/IL-24 + cisplatin-induced killing (Figure S4). Cisplatin treatment activated CD95, and this effect that was enhanced by expression of MDA-7/IL-24 (Figure 4E, inset panel). Our data demonstrate that MDA-7/IL-24-induced activation of PERK plays a key role in regulating mitochondrial stability through MCL-1 and that cisplatin enhances MDA-7/IL-24 toxicity via activation of the extrinsic pathway and *de novo* ceramide synthesis.

Finally, we determined whether Ad.5-*mda-7* interacted with another clinically relevant therapeutic agent used in OCC therapy: paclitaxel. In both OVCAR and SKOVIII cells paclitaxel interacted in an additive fashion to promote Ad.5-*mda-7* lethality (Figure 5A). Cisplatin and paclitaxel interacted to kill OVCAR cells in at least an additive fashion and the drug combination facilitated Ad.5-*mda-7* lethality significantly above that caused by the cisplatin + Ad.5-*mda-7* combination (Figure 5B). In true percentage terms, Ad.5-*mda-7* and cisplatin caused $6.2 \pm 0.1\%$ more killing than either agent alone whereas Ad.5-*mda-7* and cisplatin and paclitaxel treatment caused $22.2 \pm 2.3\%$ ($p < 0.05$) more killing than each agent alone. These findings correlated with greater levels of pro-caspase 3 and PARP1 cleavage (Figure 5B, upper inset panel). The results also correlated with further increases in BAX levels without any significant further decline in BCL-XL levels; this suggests that the apoptotic rheostat is further altered towards pro-death signaling by the treatment with paclitaxel. Cisplatin and paclitaxel facilitated Ad.5-*mda-7* lethality to kill OVCAR cells in at least a greater than additive fashion (Figure S6). In agreement with the concept that enhanced levels of BAX were causal in the elevated levels of tumor cell killing, knockdown of BAX expression significantly reduced the lethal interaction between Ad.5-*mda-7*, cisplatin and paclitaxel (Figure 5C). Collectively, the data in Figures 3-5 demonstrates that expression of MDA-7/IL-24, via Ad.5-*mda-7* or Ad.5/3-*mda-7*, enhances the toxic effects of established OCC therapeutic drugs in OCC.

Discussion.

Previous studies have noted that GST-MDA-7 (or Ad.5-*mda-7*) reduces proliferation and causes tumor cell- and transformed cell-specific killing, and radiosensitization in malignant glioma, prostate and ovarian cancer cells (Su et al, 2003; Yacoub et al, 2004; Yacoub et al 2008; Su et al, 2006; Emdad et al 2006). However, the precise signaling pathways modified by GST-MDA-7 (or Ad.5-*mda-7*) as a single agent and casually related to its cancer-specific cell killing effects in human ovarian carcinoma cells are still not well understood.

Infection of OCC with a dose of Ad.5-*mda-7* virus particles that caused profound toxicity after ~72 h correlated with strong activation of the JNK1/2 and p38 MAPK pathways as well as of PERK and eIF2 α . This treatment, in parallel, nearly abolished ERK1/2 and AKT signaling. Multiple studies using a variety of cytokine and toxic stimuli document that prolonged JNK1-3 and/or p38 MAPK activation in a wide variety of cell types can trigger cell death (Park et al, 2009; Xia et al, 1995; Matsuzawa et al, 2002). The balance between the readouts of ERK1/2 and JNK1-3 signaling may also represent a common key homeostatic mechanism that regulates cell survival versus cell death processes. Inhibition of JNK1/2 or p38 MAPK reduced MDA-7/IL-24 toxicity and inhibition of both pathways abolished killing; this was associated with reduced activation of BAX and BAK.

We have published studies arguing that signaling via PERK can promote tumor cell death or alternatively cell survival based on the stimulus (Yacoub et al, 2008b; Park et al, 2008; Zhang et al, 2008). There are three primary UPR sensors: PERK, (PKR-like ER kinase), ATF6 (activating transcription factor 6) and IRE1. As unfolded proteins accumulate, BiP (GRP78), the HSP70 ER resident chaperone, dissociates from PERK, ATF6 or IRE1. BiP/GRP78 dissociation from PERK allows this protein to dimerize, auto-phosphorylate, and then phosphorylate eukaryotic translation initiation factor alpha, the protein required for bringing the initiator methionyl-transfer RNA to the 40S ribosome (Park et al, 2008; Zhang et al, 2008, and references therein). Phosphorylated eIF2 α thus leads to repression of global translation, helping to allow cells to recover from the accumulation of unfolded proteins. Reduced translation, however, can also lower expression of some pro-

survival proteins such as MCL-1 and c-FLIP-s, as noted in OCC after expression of MDA-7/IL-24, leading to increased cell death. MDA-7/IL24 binds to BiP/GRP78 and in OCC we hypothesized that this binding would play a central role in regulating PERK activity / activation and regulating MDA-7/IL24-induced cell killing (Gupta et al, 2006a). Indeed, a constitutively active form of MEK1 maintained ERK1/2 phosphorylation in cells expressing MDA-7/IL-24, and increased BiP/GRP78 expression and blocked PERK activation. Over-expression of BiP/GRP78 blocked MDA-7/IL-24-induced PERK activation and expression of dominant negative PERK blocked MDA-7/IL-24-induced activation of JNK1/2 as well as reduced expression of MCL-1. Thus in OCC MDA-7/IL-24, by binding to BiP/GRP78, results in disruption of the BiP/GRP78-PERK chaperone interaction resulting in enhanced PERK signaling into the eIF2 α and JNK downstream pathways that act to promote mitochondrial dysfunction via decreased protective BCL-2 family protein expression and increased activity of toxic BH3 domain proteins, respectively.

In one ovarian cancer cell line MDA-7/IL-24 lethality has previously been shown to be mediated by CD95-caspase 8 signaling, indicating that the extrinsic pathway to apoptosis could be activated by this cytokine (Gopalan et al, 2005). However, in many of our prior analyses with MDA-7/IL24 in breast, prostate, pancreatic and brain tumor cells, as well as from the work of others, it was noted that MDA-7/IL-24-induced cell death was mediated by disruption of mitochondrial function with little or no involvement of death receptors or caspase 8 in the killing process. Our present studies suggest that in SKOVIII cells, but not OVCAR cells, that extrinsic pathway signaling also plays a role in MDA-7/IL-24 lethality. In renal carcinoma cells we have recently noted that over-expression of c-FLIP-s or the caspase 8 inhibitory protein CRM A blocked GST-MDA-7 lethality, and knockdown of CD95 or FADD expression also reduced GST-MDA-7 toxicity (Park et al, 2009).

In addition, to JNK pathway-mediated activation of BAX and BAK, our findings in OVCAR cells also argued that MDA-7/IL-24 caused altered ratios in the total expression of pro-apoptotic BH3 domain containing proteins, particularly BAX, and anti-apoptotic proteins, such as MCL-1 and BCL-XL, with the subsequent activation of caspases 9 and 3; this finding is similar to data obtained expressing MDA-7/IL-24 in other tumor

cell types, e.g., LNCaP prostate cancer cells (Fisher, 2005). In other prostate cancer cell types, such as DU-145, which lack expression of BAX, Ad.5-*mda-7* is an even more potent inducer of tumor cell death than is observed in LNCaP cells. In GBM cells, our prior data argued that at least 5 BH3 domain-containing proteins could potentially mediate GST-MDA-7 toxicity downstream of GST-MDA-7-stimulated activation of PERK and JNK1-3 (Yacoub et al, 2008a; Yacoub et al, 2008b). Collectively, based on these findings, it is probable that the reason why multiple transformed cell types exhibit MDA-7/IL-24 toxicity regardless of their genetic background is due to the pleiotropic range of pro-apoptotic proteins and pathways that can be recruited by this cytokine to initiate mitochondrial cell death processes.

Platinum based chemotherapeutic drugs are a mainstay of ovarian cancer therapy (Coleman and Sood, 2006). MDA-7/IL-24 and cisplatin, as well as a novel Pt containing drug BBR3464, interacted in a greater than additive fashion to kill OCCs *in vitro* via CD95. In prior work, treating primary hepatocytes with low doses of bile acids, which cause ligand independent activation of CD95, we discovered that JNK1/2 activation was CD95-dependent and our recent studies in renal carcinoma cells also demonstrated that JNK1/2 and to a lesser extent p38 MAPK activation following GST-MDA-7 treatment required CD95 signaling. In OCC cisplatin further enhanced MDA-7/IL-24-induced JNK1/2 activation, and this enhanced JNK1/2 activation was required for the toxic interaction between the two agents. MDA-7/IL-24-induced PERK activation was required for MDA-7/IL-24 and MDA-7/IL-24 + cisplatin-induced JNK1/2 and p38 MAPK activation. Matsuzawa et al. have previously implicated a TRAF2-ASK1-JNK cascade downstream of IRE1 in ER-stress responses in multiple cell types, and based on our data PERK-dependent signaling could also feed into this cell survival regulatory process (Matsuzawa et al, 2002). Further studies are necessary to determine if the enhanced activity of MDA-7/IL24, when administered by an oncolytic adenovirus, with cisplatin in the context of hepatocellular carcinoma (Wu et al, 2009) involve similar signaling pathway alterations as observed in OCC.

In our recent studies treating primary hepatocytes with bile acids; in RCC / HCC / pancreatic tumor cells with the drugs sorafenib and vorinostat; and in renal carcinoma cells treated with GST-MDA-7 we discovered that

ligand-independent activation of CD95 was dependent in part on the actions of ASMase and the *de novo* ceramide synthesis pathway (Park et al, 2008; Zhang et al, 2008). Recent studies have suggested that the *de novo* and ASMase pathways of ceramide generation can cooperate to regulate lipid raft function (Zhang et al, 2008a); cisplatin was shown to promote CD95 activation and that ceramide generation may play a role in this process (Min et al, 2007). The molecular mechanisms by which MDA-7/IL-24 enhances cisplatin-induced activation of CD95, and whether cisplatin-induced DNA damage increases expression of ceramide synthase genes, will require studies beyond the scope of the present manuscript.

The studies in the present manuscript were also to determine whether we could enhance the infectivity of adenoviral gene transduction in OCC, using a chimeric adenovirus containing the knob protein expressing portions of the type 5 and type 3 adenoviruses. A type 5/3 recombinant adenovirus was more efficacious at delivering *mda-7/IL-24* to tumor cells than a type 5 virus, resulting in greater expression of MDA-7/IL-24. The greater expression of MDA-7/IL-24 using the type 5/type 3 virus resulted in a greater amount of tumor cell killing, as observed using this virus in low CAR prostate cancer cells (Dash et al, 2009). Of note, however, was that while infection using Ad.5/3-*mda-7* generated at least 10-fold more MDA-7/IL-24 protein it only enhanced apoptosis ~3-fold more than Ad.5-*mda-7* infection. This argues that there is a certain threshold at which MDA-7/IL-24 becomes toxic to a tumor cell and producing more MDA-7/IL-24 may not *per se* increase killing. We have observed a similar dose-dependent effect of GST-MDA-7 on GBM and renal carcinoma cells *in vitro* (Yacoub et al, 2008b; Park et al, 2009). However, based on the pleiotropic anti-tumor effects of MDA-7/IL-24 *in vivo*, including inhibition of tumor angiogenesis, potent ‘bystander’ anti-cancer activity and immune modulating activity, having enhanced expression of MDA-7/IL-24 may directly contribute to and enhance the anti-cancer properties of this cytokine *in vivo* (Fisher, 2005; Emdad et al, 2009; Sarkar et al, 2005; Sarkar et al, 2007; Sarkar et al, 2008; Sauane et al, 2008; Greco et al, 2009).

References

Caudell EG, Mumm JB, Poindexter N, et al. The protein product of the tumor suppressor gene, melanoma differentiation-associated gene 7, exhibits immunostimulatory activity and is designated IL-24. *J Immunol* 2002; 168: 6041-6046.

Chada S, Bocangel D, Ramesh R, et al. *mda-7/IL24* kills pancreatic cancer cells by inhibition of the Wnt/PI3K signaling pathways: identification of IL-20 receptor-mediated bystander activity against pancreatic cancer. *Mol Ther* 2005; 11: 724-733.

Coleman RL, Sood AK. Historical progress in the initial management of ovarian cancer: intraperitoneal chemotherapy. *Curr Oncol Rep* 2006; 8:455-464.

Cunningham CC, Chada S, Merritt JA, et al. Clinical and local biological effects of an intratumoral injection of *mda-7* (IL24; INGN 241) in patients with advanced carcinoma: a phase I study. *Mol Ther* 2005; 11: 149-159.

Dash R, Dmitriev IP, Su Z-z, et al. Enhanced delivery of *mda-7/IL-24* using a serotype chimeric adenovirus (Ad.5/3) improves therapeutic efficacy in low CAR prostate cancer cells. *Cancer Gene Ther* 2009, in press.

Ekmekcioglu S, Ellerhorst J, Mhashilkar AM, et al. Down-regulated melanoma differentiation associated gene (*mda-7*) expression in human melanomas. *Int J Cancer* 2001; 94: 54-59.

Ellerhorst JA, Prieto VG, Ekmekcioglu S. Loss of MDA-7 expression with progression of melanoma. *J Clin Oncol* 2002; 20: 1069-1074.

Emdad L, Sarkar D, Lebedeva IV, et al. Ionizing radiation enhances adenoviral vector expressing *mda-7/IL-24*-mediated apoptosis in human ovarian cancer. *J Cell Physiol* 2006; 208: 298-306.

Emdad L, Lebedeva IV, Su Z-z, et al. Historical perspective and recent insights into our understanding of the molecular and biochemical basis of the antitumor properties of *mda-7/IL-24*. *Cancer Biol & Ther* 2009; 8: 391-400.

Fisher PB, Gopalkrishnan RV, Chada S, et al. *mda-7/IL-24*, a novel cancer selective apoptosis inducing cytokine gene: from the laboratory into the clinic. *Cancer Biol Ther* 2003; 2: S23-37.

Fisher PB, Sarkar D, Lebedeva IV, et al. Melanoma differentiation associated gene-7/interleukin-24 (*mda-7/IL-24*): novel gene therapeutic for metastatic melanoma. *Toxicol & Applied Pharmacol* 2007; 224: 300-307.

Fisher PB. Is *mda-7/IL-24* a "magic bullet" for cancer? *Cancer Res* 2005; 65: 10128-10138.

Gopalan B, Litvak A, Sharma S, Mhashilkar AM, Chada S, Ramesh R. Activation of the Fas-FasL signaling pathway by MDA-7/IL-24 kills human ovarian cancer cells. *Cancer Res* 2005; 65: 3017-3024.

Greco A, Di Benedetto A, Howard CM, et al. Eradication of therapy-resistant human prostate tumors using an ultrasound guided site-specific cancer terminator virus delivery approach. *Mol Ther* 2009, in press.

Guicciardi ME, Deussing J, Miyoshi H, et al. Cathepsin B contributes to TNF-alpha-mediated hepatocyte apoptosis by promoting mitochondrial release of cytochrome c. *J Clin Invest* 2000; 106: 1127-1137.

Gupta P, Walter MR, Su ZZ, et al. BiP/GRP78 Is an intracellular target for MDA-7/IL-24 induction of cancer-specific apoptosis. *Cancer Res* 2006b; 66: 8182-8191.

Gupta P, Su ZZ, Lebedeva IV, et al. *mda-7/IL-24*: multifunctional cancer-specific apoptosis-inducing cytokine. *Pharmacol Ther* 2006a; 111: 596-628.

Huang EY, Madireddi MT, Gopalkrishnan RV, et al. Genomic structure, chromosomal localization and expression profile of a novel melanoma differentiation associated (*mda-7*) gene with cancer specific growth suppressing and apoptosis inducing properties. *Oncogene* 2001; 20: 7051-7063.

Jiang H, Lin JJ, Su ZZ, Goldstein, NI, Fisher, PB. Subtraction hybridization identifies a novel melanoma differentiation associated gene, *mda-7*, modulated during human melanoma differentiation, growth and progression. *Oncogene* 1995; 11: 2477-2486.

Lebedeva IV, Su ZZ, Chang Y, Kitada S, Reed JC, Fisher PB. The cancer growth suppressing gene *mda-7* induces apoptosis selectively in human melanoma cells. *Oncogene* 2002; 21: 708-718.

Lebedeva IV, Sarkar D, Su Z-z, et al. Bcl-2 and Bcl-x_L differentially protect human prostate cancer cells from induction of apoptosis by melanoma differentiation associated gene-7, *mda-7/IL-24*. *Oncogene* 2003; 22: 8758-8773.

Lebedeva IV, Sauane M, Gopalkrishnan RV, et al. *mda-7/IL-24*: exploiting cancer's Achilles' heel. *Mol Ther* 2005; 11: 4-18.

Matsuzawa A, Nishitoh H, Tobiume K, Takeda K, Ichijo H. Physiological roles of ASK1-mediated signal transduction in oxidative stress- and endoplasmic reticulum stress-induced apoptosis: advanced findings from ASK1 knockout mice. *Antioxid Redox Signal* 2002; 4: 415-425.

Mhashilkar AM, Stewart AL, Sieger K, et al. MDA-7 negatively regulates the beta-catenin and PI3K signaling pathways in breast and lung tumor cells. *Mol Ther* 2003; 8: 207-219.

Min J, Mesika A, Sivaguru M, Van Veldhoven PP, Alexander H, Futerman AH, Alexander S. (Dihydro)ceramide synthase 1 regulated sensitivity to cisplatin is associated with the activation of p38 mitogen-activated protein kinase and is abrogated by sphingosine kinase 1. *Mol Cancer Res* 2007; 5:801-12.

Park MA, Zhang G, Martin AP, et al. Vorinostat and sorafenib increase ER stress, autophagy and apoptosis via ceramide-dependent CD95 and PERK activation. *Cancer Biol Ther* 2008; **7**: in press.

Park MA, Walker T, Martin AP, et al. MDA-7/IL-24-induced cell killing in malignant renal carcinoma cells occurs by a ceramide/CD95/PERK-dependent mechanism. *Mol Cancer Ther*. 2009 May 5. [Epub ahead of print]

Parrish-Novak J, Xu W, Brender T, et al. Interleukins 19, 20, and 24 Signal through Two Distinct Receptor Complexes. Differences in receptor-ligand interactions mediate unique biological functions. *J Biol Chem* 2002; 277: 47517-47523.

Pestka S, Krause CD, Sarkar D, Walter MR, Shi Y, Fisher PB. Interleukin-10 and related cytokines and receptors. *Annu Rev Immunol* 2004; 22: 929-979.

Sarkar D, Su ZZ, Lebedeva IV, et al. *mda-7* (IL-24) Mediates selective apoptosis in human melanoma cells by inducing the coordinated over-expression of the GADD family of genes by means of p38 MAPK. *Proc Natl Acad Sci USA* 2002; 99: 10054-10059.

- Sarkar D, Su Z-z, Vozhilla N, et al. Dual cancer-specific targeting strategy cures primary and distant breast carcinomas in nude mice. *Proc Natl Acad Sci USA* 2005; 102: 14034-14039.
- Sarkar D, Lebedeva IV, Su Z-z, et al. Eradication of therapy resistant human prostate tumors using a cancer terminator virus. *Cancer Res* 2007; 67: 5434-5442.
- Sarkar D, Su Z-z, Park E-S, et al. A cancer terminator virus (CTV) eradicates both treated primary and untreated distant human melanomas. *Cancer Gene Ther* 2008; 15: 293-302.
- Sauane M, Gopalkrishnan RV, Choo HT, et al. Mechanistic aspects of *mda-7/IL-24* cancer cell selectivity analysed via a bacterial fusion protein. *Oncogene*. 2004; 23: 7679-7690.
- Sauane M, Su Z-z, Gupta P, et al. Autocrine regulation of *mda-7/IL-24* mediates cancer-specific apoptosis. *Proc Natl Acad Sci USA* 2008; 105: 9763-9768.
- Staudt MR, DePass AL, Sarkar D, Fisher PB. Model cell culture system for defining the molecular and biochemical events mediating terminal differentiation of human melanoma cells. *J Cell Physiol* 2009; 218: 304-318.
- Su ZZ, Lebedeva IV, Gopalkrishnan RV, et al. A combinatorial approach for selectively inducing programmed cell death in human pancreatic cancer cells. *Proc Natl Acad Sci USA* 2001; 98: 10332-10337.
- Su ZZ, Madireddi MT, Lin JJ, et al. The cancer growth suppressor gene *mda-7* selectively induces apoptosis in human breast cancer cells and inhibits tumor growth in nude mice. *Proc Natl Acad Sci USA* 1998; 95: 14400-14405.

- Su ZZ, Lebedeva IV, Sarkar D, et al. Ionizing radiation enhances therapeutic activity of *mda-7/IL-24*: overcoming radiation- and *mda-7/IL-24*-resistance in prostate cancer cells over-expressing the antiapoptotic proteins bcl-x_L or bcl-2. *Oncogene* 2006; 25: 2339-2348.
- Wu YM, Zhang KJ, Yue XT, et al. Enhancement of tumor cell death by combining cisplatin with an oncolytic adenovirus carrying MDA-7/IL-24. *Acta Pharmacol Sin* 2009; 30: 467-477.
- Xia Z, Dickens M, Raingeaud J, Davis RJ, Greenberg ME. Opposing effects of ERK and JNK-p38 MAP kinases on apoptosis. *Science* 1995; 270: 1326-1331.
- Yacoub A, Mitchell C, Hong Y, et al. MDA-7 regulates cell growth and radiosensitivity in vitro of primary (non-established) human glioma cells. *Cancer Biol Ther* 2004; 3: 739-751.
- Yacoub A, Hamen H, Emdad L, et al. MDA-7/IL-24 plus radiation enhance survival in animals with intracranial primary human GBM tumors. *Cancer Biol Ther* 2008; 7: 917-933.
- Yacoub A, Park MA, Gupta P, et al. Caspase-, cathepsin-, and PERK-dependent regulation of MDA-7/IL-24-induced cell killing in primary human glioma cells. *Mol Cancer Ther* 2008a; 7: 297-313.
- Yacoub A, Gupta P, Park MA, et al. Regulation of GST-MDA-7 toxicity in human glioblastoma cells by ERBB1, ERK1/2, PI3K, and JNK1-3 pathway signaling. *Mol Cancer Ther*. 2008b; 7: 314-329.
- Yacoub A, Mitchell C, Brannon J, et al. MDA-7 (interleukin-24) inhibits the proliferation of renal carcinoma cells and interacts with free radicals to promote cell death and loss of reproductive capacity. *Mol Cancer Ther* 2003; 2: 623-632.

Zhang G, Park MA, Mitchell C, et al. Multiple cyclin kinase inhibitors promote bile acid-induced apoptosis and autophagy in primary hepatocytes via p53-CD95-dependent signaling. *J Biol Chem* 2008; 283: 24343-24358.

Zhang Y, Li X, Becker KA, Gulbins E. Ceramide-enriched membrane domains-Structure and function. *Biochim Biophys Acta*. 2008a, in press.

Footnotes.

Support for the present study was provided from PHS grants: P01-CA104177, R01-CA108325, R01-DK52825; R01-CA63753; R01-CA77141; R01-CA097318; R01-CA127641-01; P01-NS031492, The V Foundation and The Samuel Waxman Cancer Research Foundation. P.D. is The Universal Inc. Professor in Signal Transduction Research; D.S. is the Harrison Endowed Scholar in the VCU Massey Cancer Center; P.B.F. holds the Thelma Newmeyer Corman Chair in Cancer Research at the VCU Massey Cancer Center and is a SWCRF Investigator.

Figure Legends

Figure 1. MDA-7/IL-24 causes a dose-dependent induction of growth arrest and OCC death. Panels A. and B. OVCAR cells and SKOVIII cells were treated 24 h after plating with GST-MDA-7 (0-200 nM). At the indicated time point after GST-MDA-7 treatment (96 h), cell viability was determined by trypan blue exclusion assay and cell numbers were determined using hemocytometer (\pm SEM, n = 3). **Panel C.** OVCAR and SKOVIII cells were infected with type 5 recombinant adenoviruses empty vector (Ad.5-*cmv*) or to express MDA-7/IL-24 (Ad.5-*mda-7*) at 20 or 80 m.o.i. Cells were isolated 48 h after exposure and the loss of cell viability above empty vector Ad.5-*cmv* infection determined by using Annexin V Propidium iodide staining assays in triplicate using a flow cytometer (\pm SEM, n = 3).

Figure 2. MDA-7/IL-24 promotes transformed cell killing through ER stress signaling and activation of the JNK/p38 MAPK pathways. Panel A. OVCAR cells were infected with Ad.5-*cmv* or Ad.5-*mda-7* at 50 m.o.i. Cells were isolated 12-48 h after infection and processed for SDS PAGE and immunoblotting against the indicated proteins (n = 3). **Panel B.** OVCAR cells were transfected with empty vector plasmid (CMV) or with a plasmid to express dominant negative PERK. Twelve h after transfection cells were infected with Ad.5-*cmv* or Ad.5-*mda-7* at 50 m.o.i. Cells were isolated 48 h after infection and processed for SDS PAGE and immunoblotting against the indicated proteins (n = 3). **Panel C.** OVCAR and SKOV3 cells were infected at an m.o.i. of 50 and 100, respectively, with Ad.5-*cmv* or Ad.5-*mda-7*. In parallel as indicated, cells were infected with a virus to express dominant negative p38 MAPK. Twenty four h after infection cells were treated with vehicle or with JNK-IP (10 μ M). At the indicated time points in the graphs, cells were isolated and the loss of cell viability determined by trypan blue exclusion assays in triplicate (\pm SEM, n = 3). **Panel D.** OVCAR cells were infected with viruses and treated with JNK-IP as in *Panel C.* Forty eight h after infection, cells were isolated and portions of the lysates subjected to immunoprecipitation for isolation of activated forms of BAX and BAK. The precipitates were subjected to SDS PAGE alongside an equal portion of the total cell lysates and blotting performed to determine the

levels of BAX, BAK and GAPDH (n = 2). **Panel E.** OVCAR and SKOVIII cells were infected at an m.o.i. of 50 and 100, respectively, with Ad.5-*cmv* or Ad.5-*mda-7*. In parallel as indicated, cells were infected with recombinant adenoviruses to express activated and dominant negative forms of AKT and MEK1, or with viruses to express apoptosis inhibitory proteins (c-FLIP-s, BCL-XL, dominant negative caspase 9). Treatment with LY294002 (10 μ M) occurred 24 h after virus infection. At the indicated time points in the graphs, cells were isolated and the loss of cell viability determined by trypan blue exclusion assays in triplicate (\pm SEM, n = 3). **Panel F.** OVCAR cells were transfected as indicated with expression plasmids (empty vector CMV, dominant negative PERK, BiP/GRP78, MCL-1) or with siRNA (siSCR, siATG5) and 12 h after transfection cells were infected with Ad.5-*cmv* or Ad.5-*mda-7* at 50 m.o.i. Cells were isolated 72 h after infection and the loss of cell viability determined by trypan blue exclusion assays in triplicate (\pm SEM, n = 3).

Figure 3. A tropism modified type 5 / type 3 virus infects ovarian cancer cells more readily than a type 5 virus, and enhances cisplatin toxicity. Panel A. OVCAR and SKOVIII cells were infected with Ad.5-*cmv* or Ad.5-*mda-7* or with tropism modified viruses Ad.5/3-*cmv* or Ad.5/3-*mda-7* at 20 or 80 m.o.i., as indicated. Cells were isolated 48 h after infection and the loss of cell viability determined by trypan blue exclusion assays in triplicate (\pm SEM, n = 3). *Inset Panel:* cells were infected with the indicated viruses and 24h after infection cells were isolated to determine the expression of MDA-7/IL-24 and the cleavage status of PARP1. **Panel B.** OVCAR and SKOVIII cells were infected with Ad.5-*cmv* or Ad.5-*mda-7* or with tropism modified viruses Ad.5/3-*cmv* or Ad.5/3-*mda-7* at 80 m.o.i. Twenty four h after infection cells were treated with vehicle or cisplatin (CDDP, 3 μ M). Seventy two h after infection cells were isolated and the loss of cell viability determined by trypan blue exclusion assays in triplicate (\pm SEM, n = 3). *Inset Panel:* identical portions of OVCAR cells, infected as indicated, were isolated 72 h after exposure and the loss of cell viability determined by using Annexin V Propidium iodide staining assays in triplicate using a flow cytometer (\pm SEM, n = 3). **Panel C.** OVCAR and SKOVIII cells were infected with Ad.5-*cmv* or Ad.5-*mda-*

7 at 80 m.o.i. and 24 h after infection cells were treated with vehicle or BBR3464 (BBR3464, 100-300 nM). Forty eight h after infection cells were isolated and the loss of cell viability determined by trypan blue exclusion assays in triplicate (\pm SEM, n = 3). **Panel D.** OVCAR cells were plated in sextuplicate as single cells were infected with Ad.5-*cmv* or Ad.5-*mda-7* at 80 m.o.i. and 24h after infection cells were treated with vehicle or cisplatin (CDDP, 3 μ M). The media was changed to drug free media 48 h after CDDP treatment and colonies permitted to form for 10-14 days (\pm SEM, n = 2).

Figure 4. Ad.5-*mda-7* + cisplatin toxicity in OCCs is dependent on PERK, JNK and CD95 signaling.

Panel A. OVCAR cells were infected with Ad.5-*cmv* or Ad.5-*mda-7* in parallel with Ad.*cmv*, Ad.*MEK1 EE* or Ad.*dnMEK1*. Twenty four h after infection cells were treated with vehicle or CDDP (3 μ M). Forty eight h after infection cells were isolated and processed for SDS PAGE and immunoblotting against the indicated proteins (n = 3). **Panel B.** OVCAR and SKOVIII cells were infected with the indicated viruses, at the stated m.o.i. and 24 h after infection cells were treated with vehicle or cisplatin (CDDP, 3 μ M). Cells were isolated 72 h after infection and the loss of cell viability determined by trypan blue exclusion assays in triplicate (\pm SEM, n = 3). **Panel C.** OVCAR cells were infected with Ad.5-*cmv* or Ad.5-*mda-7* at 80 m.o.i. in parallel with viruses to express dominant negative caspase 9, BCL-XL, or dominant negative p38 MAPK. In parallel cells were transfected with empty vector plasmid or plasmid to express Grp78/BiP. Twenty four h after infection as indicated cells were treated with JNK-IP (10 μ M) followed by cisplatin treatment (CDDP, 3 μ M). Cells were isolated 72 h after infection and the loss of cell viability determined by trypan blue exclusion assays in triplicate (\pm SEM, n = 3). *Inset Panel:* Cells infected to express MDA-7/IL-24 and/or BiP/GRP78 were isolated 48 h after infection and processed for SDS PAGE and blotting to determine the expression of MCL-1, c-FLIP-s and GAPDH and the phosphorylation of PERK. **Panel D.** OVCAR cells were infected and treated with cisplatin in an identical fashion to *Panel C*. Cells were isolated 72 h after infection and the loss of cell viability determined by using Annexin V Propidium iodide staining assays in triplicate using a flow cytometer (\pm SEM, n = 3). **Panel E.** OVCAR cells were infected with caspase 8

inhibitors (c-FLIP-s, CRM A), dominant negative p38 MAPK or transfected to express dominant negative PERK or to knockdown ceramide synthase 6 (LASS6). Twenty four h after infection cells were indicated were treated with JNK-IP (10 μ M). Cells were isolated 72 h after infection and the loss of cell viability determined by trypan blue exclusion assays in triplicate (\pm SEM, n = 3). *Inset Panel:* OVCAR cells growing in glass chambered slides in triplicate were infected to express MDA-7/IL-24 and were treated 24 h after infection with CDDP (3 μ M) for 6 h. Cells were fixed but not permeabilized and the levels of cell surface CD95 determined by immunohistochemistry (\pm SEM, n = 2).

Figure 5. Paclitaxel enhances the toxicity of [Ad.5-*mda-7* + cisplatin] in a greater than additive fashion. Panel A. OVCAR and SKOVIII cells were infected with Ad.5-*cmv* or Ad.5-*mda-7* at 80 m.o.i. Twenty four h after infection as indicated cells were treated with paclitaxel (paclitx., 0-100 nM). Cells were isolated 48 h after infection and the loss of cell viability determined by trypan blue exclusion assays in triplicate (\pm SEM, n = 3). **Panel B.** OVCAR cells were infected with Ad.5-*cmv* or Ad.5-*mda-7* at 80 m.o.i. Twenty four h after infection as indicated cells were treated with paclitaxel (paclitx., 10 nM) and/or cisplatin (CDDP, 3 μ M), as indicated. Cells were isolated 48 h after infection and the loss of cell viability determined by trypan blue exclusion assays in triplicate (\pm SEM, n = 3). Upper inset panel: cells were isolated 24 h after virus infection and processed for SDS PAGE and immunoblotting against the indicated proteins to determine expression / phosphorylation (n = 2). **Panel C.** OVCAR cells were transfected with scrambled siRNA (siSCR) or an siRNA to knock down BAX expression and 24 h later infected with Ad.5-*cmv* or Ad.5-*mda-7* at 80 m.o.i. Twenty four h after infection as indicated cells were treated with paclitaxel (paclitx., 10 nM) and cisplatin (CDDP, 3 μ M), as indicated. Cells were isolated 48 h after infection and the loss of cell viability determined by trypan blue exclusion assays in triplicate (\pm SEM, n = 3).

Figure 1A

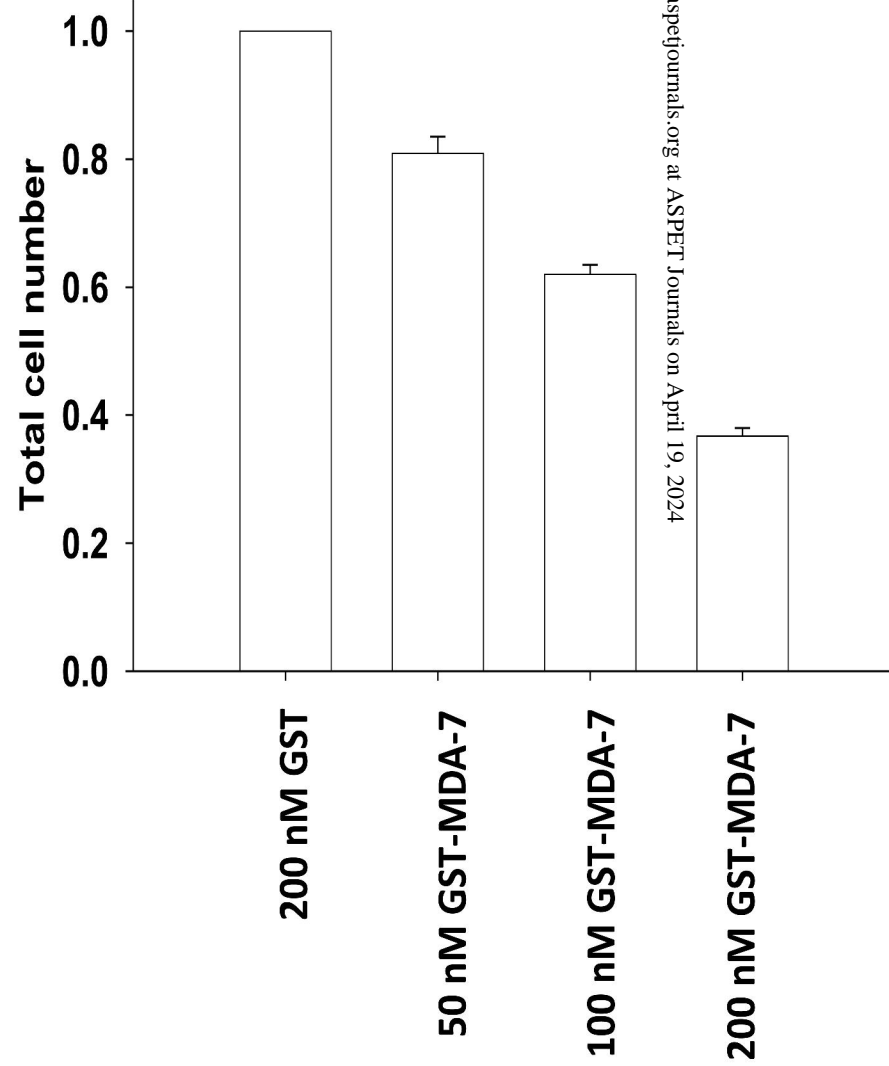
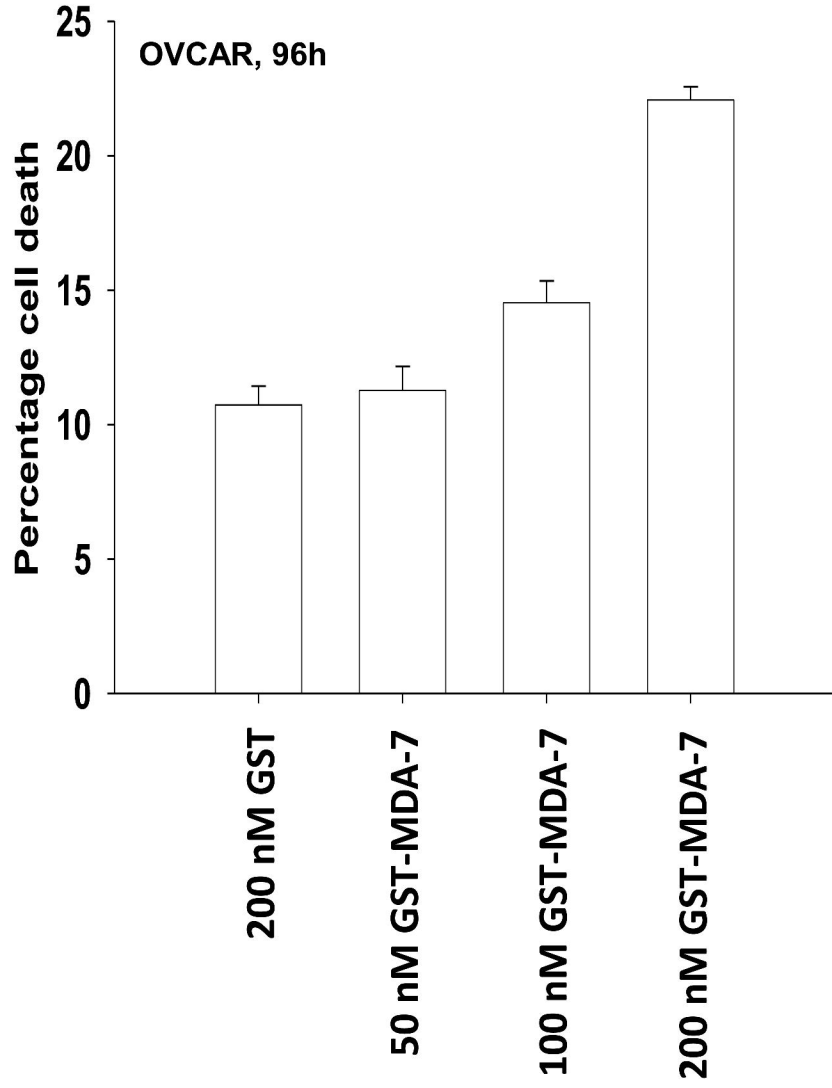


Figure 1B

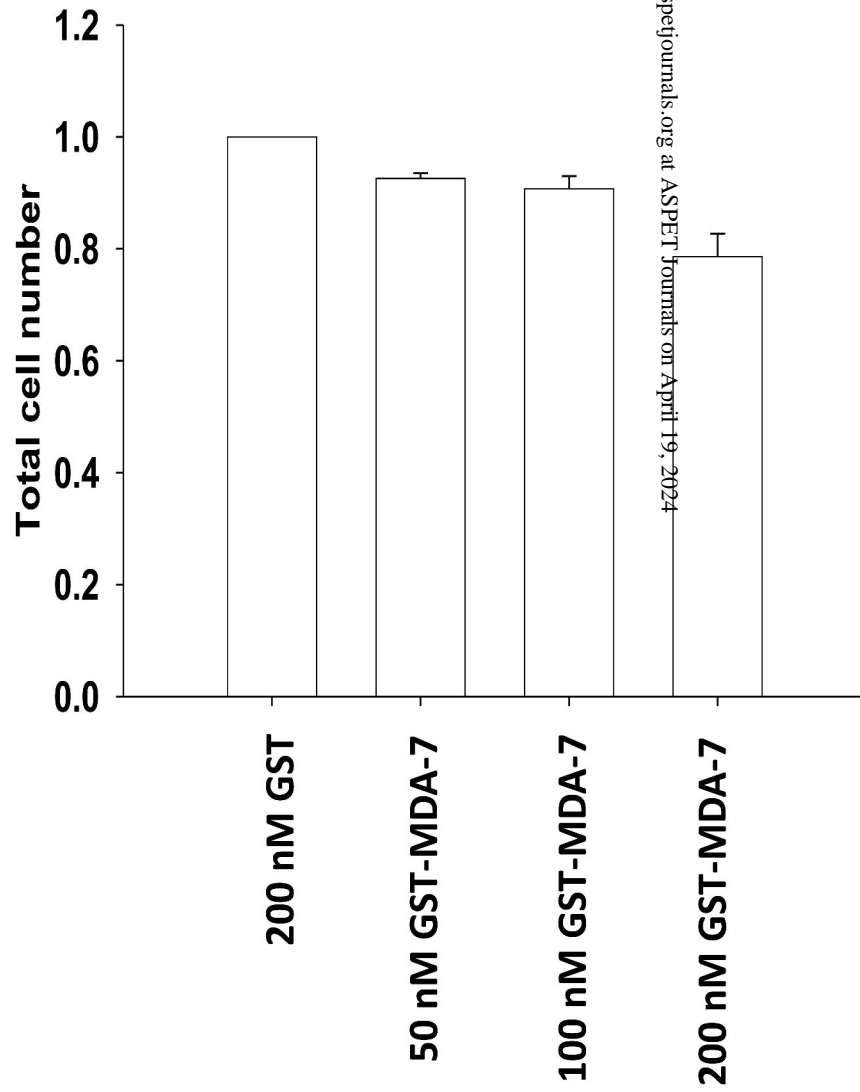
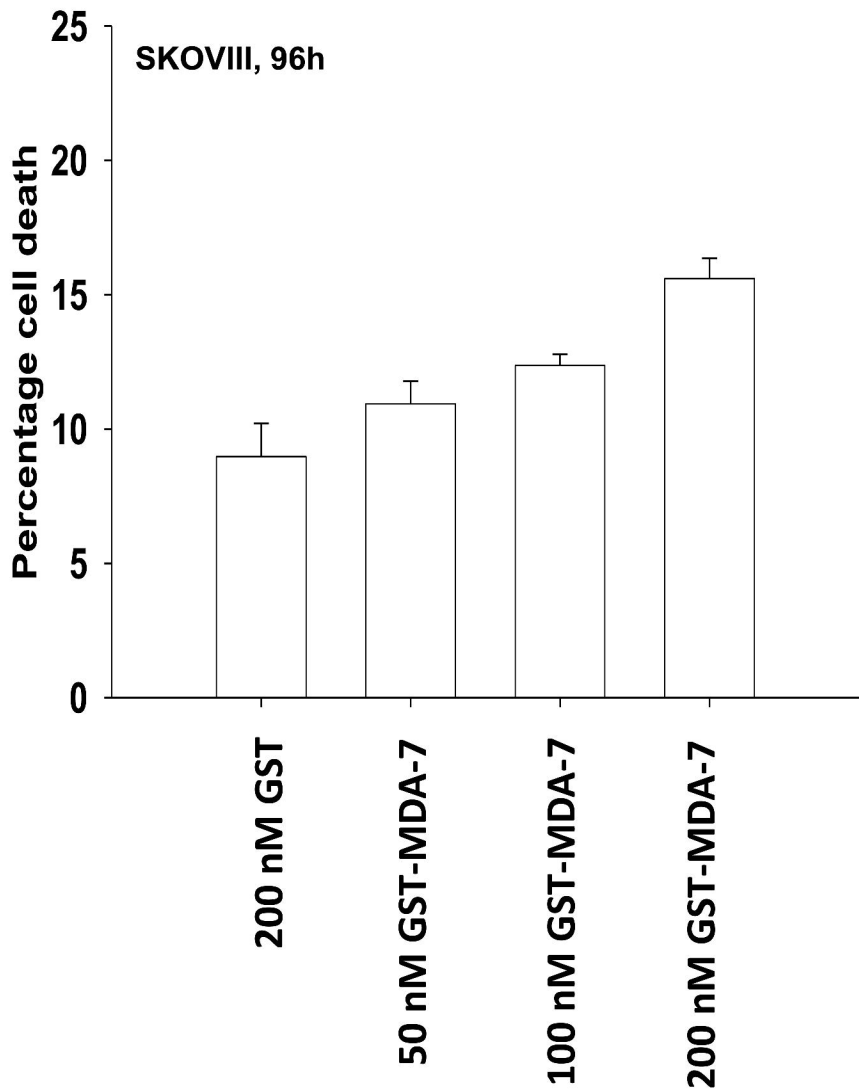


Figure 1C

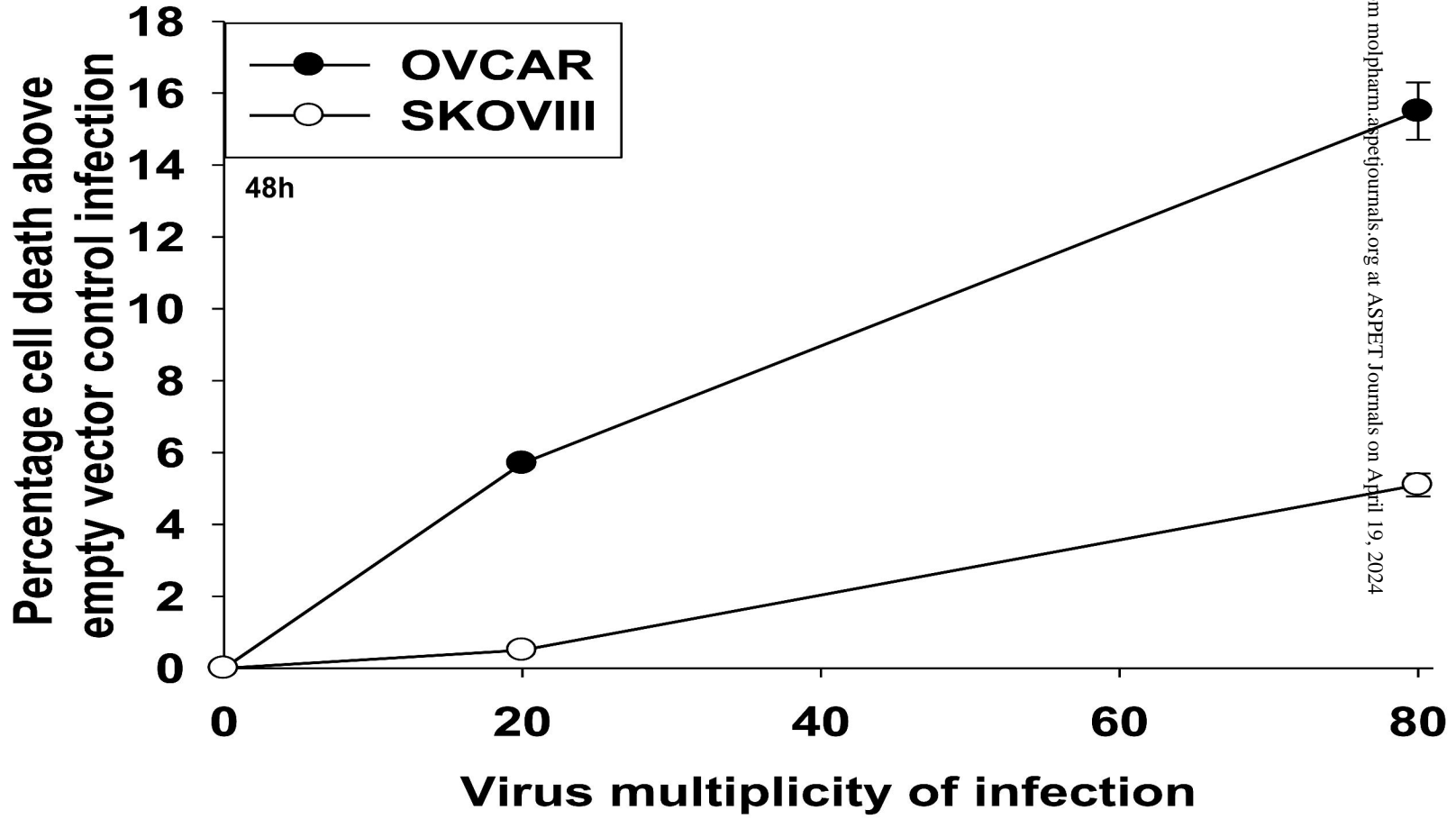


Figure 2A

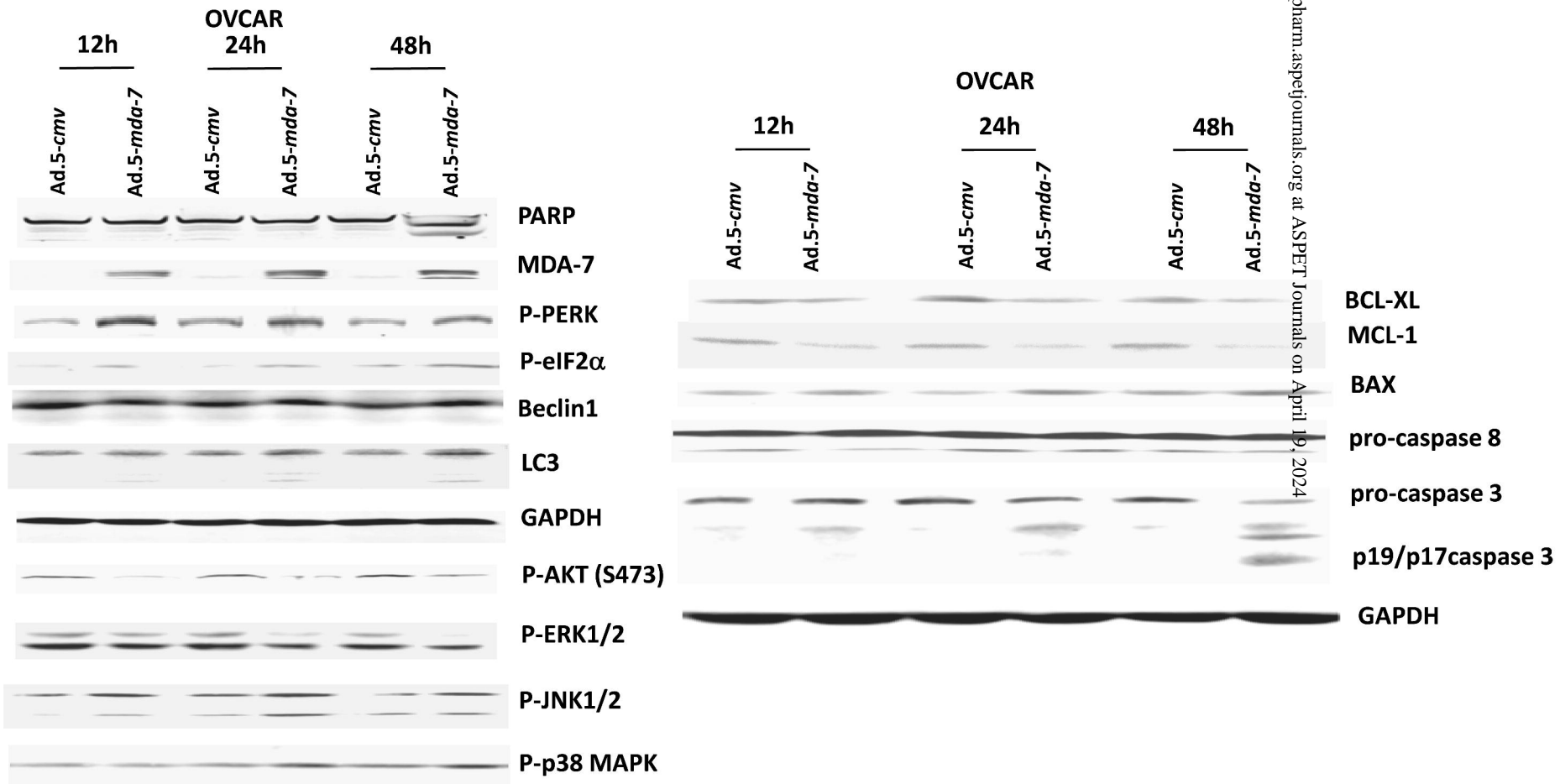


Figure 2B

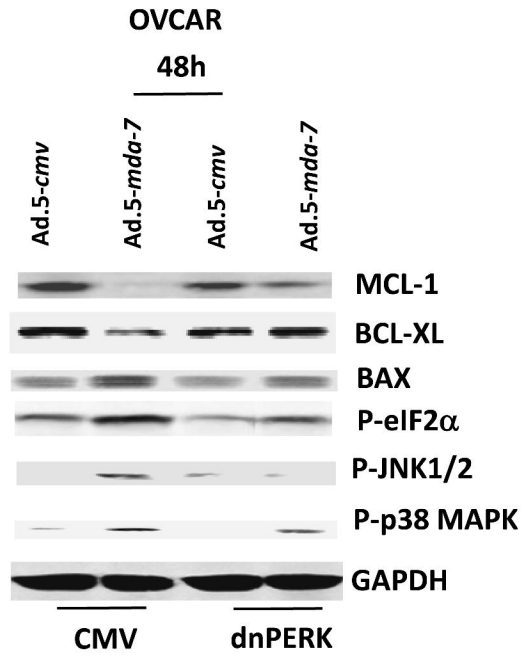


Figure 2C

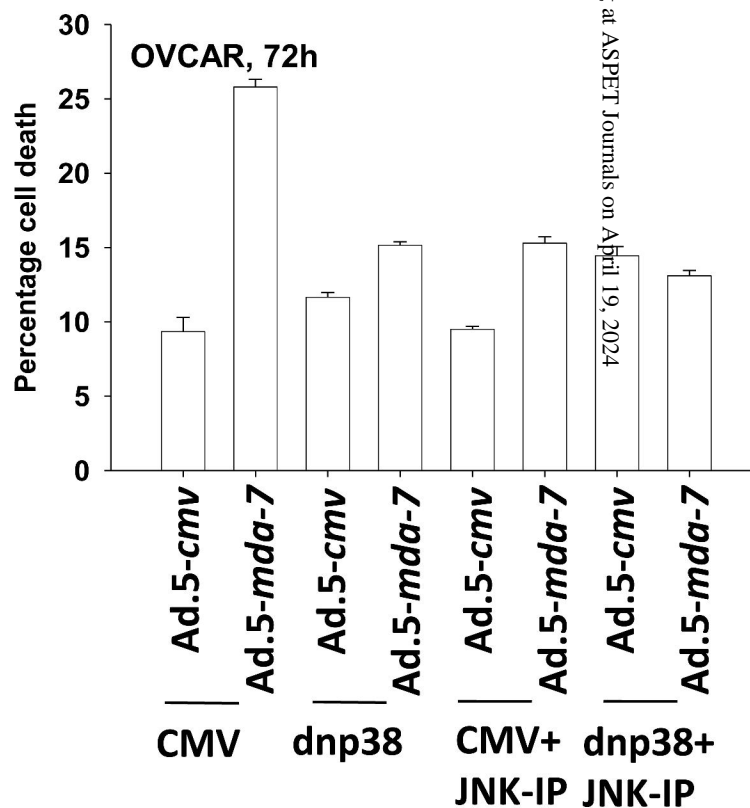
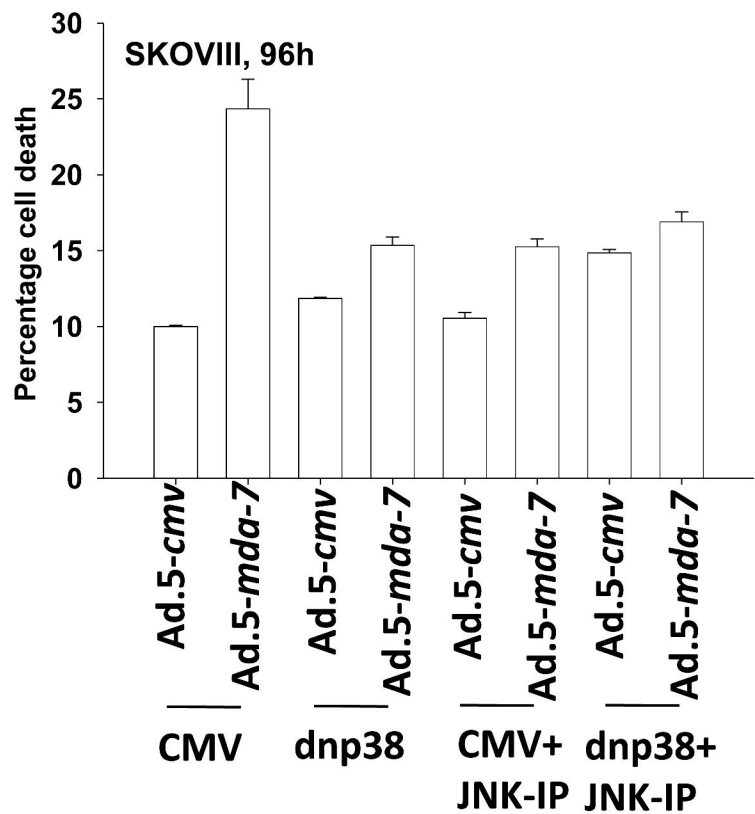


Figure 2D

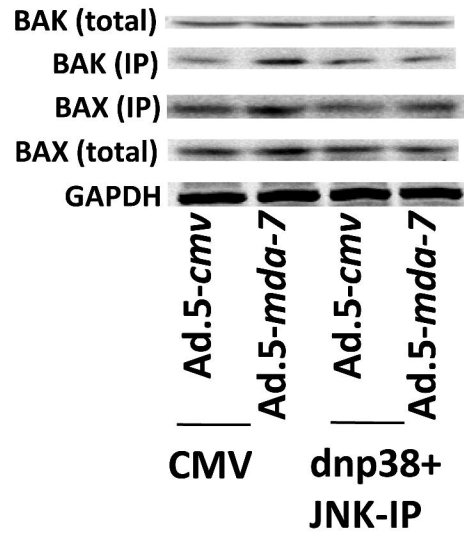
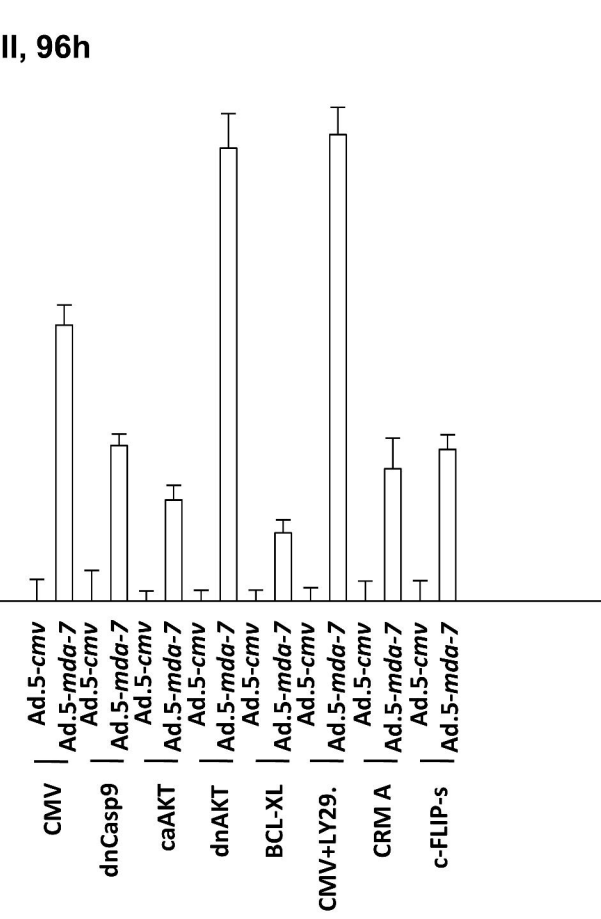


Figure 2E

Percentage cell death above vehicle control

SKOVIII, 96h



OVCAR, 72h

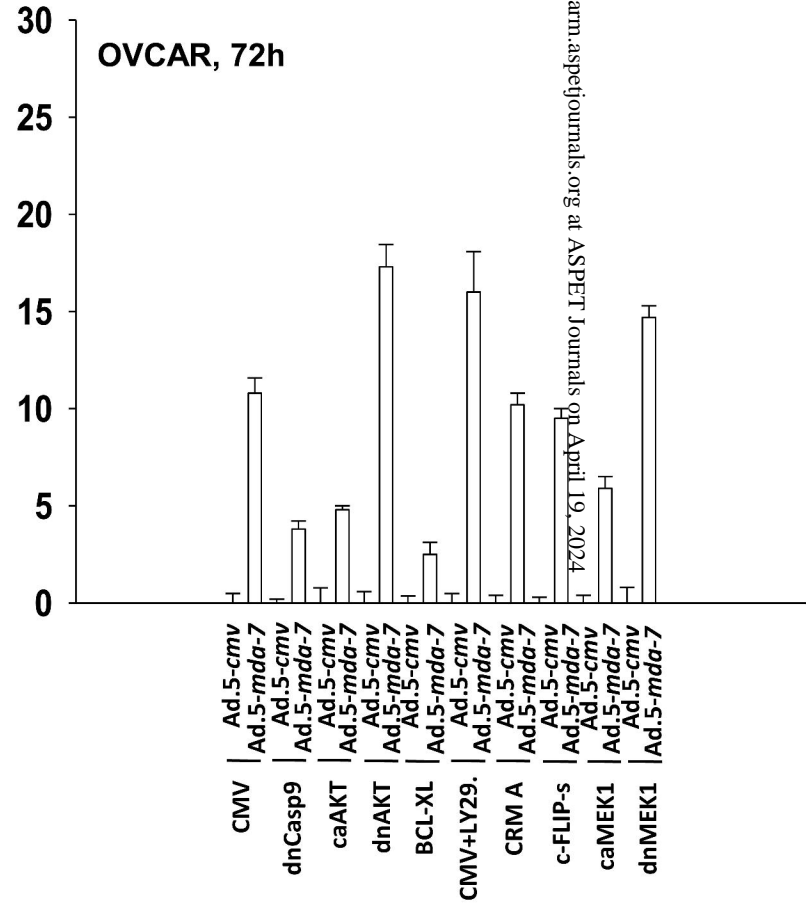


Figure 2F

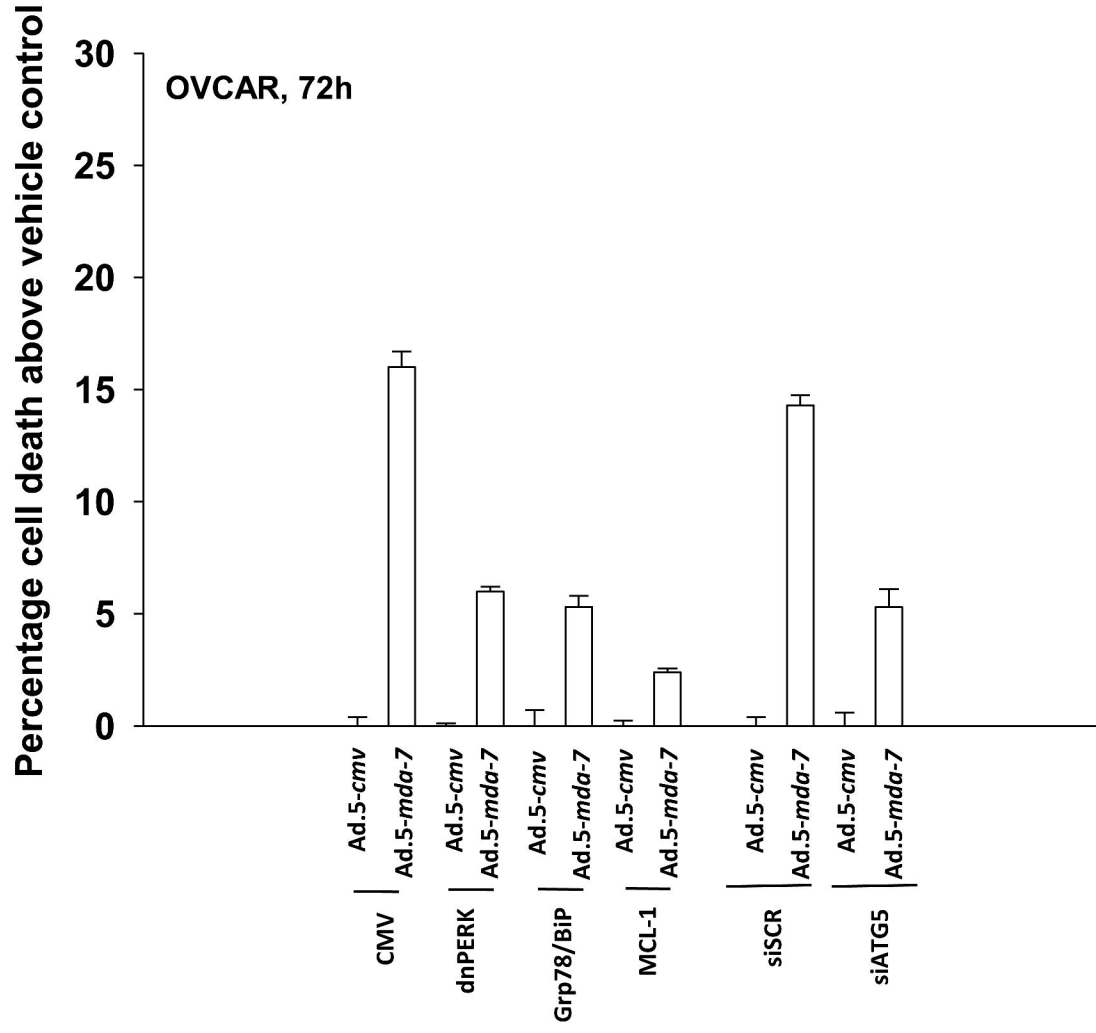


Figure 3A

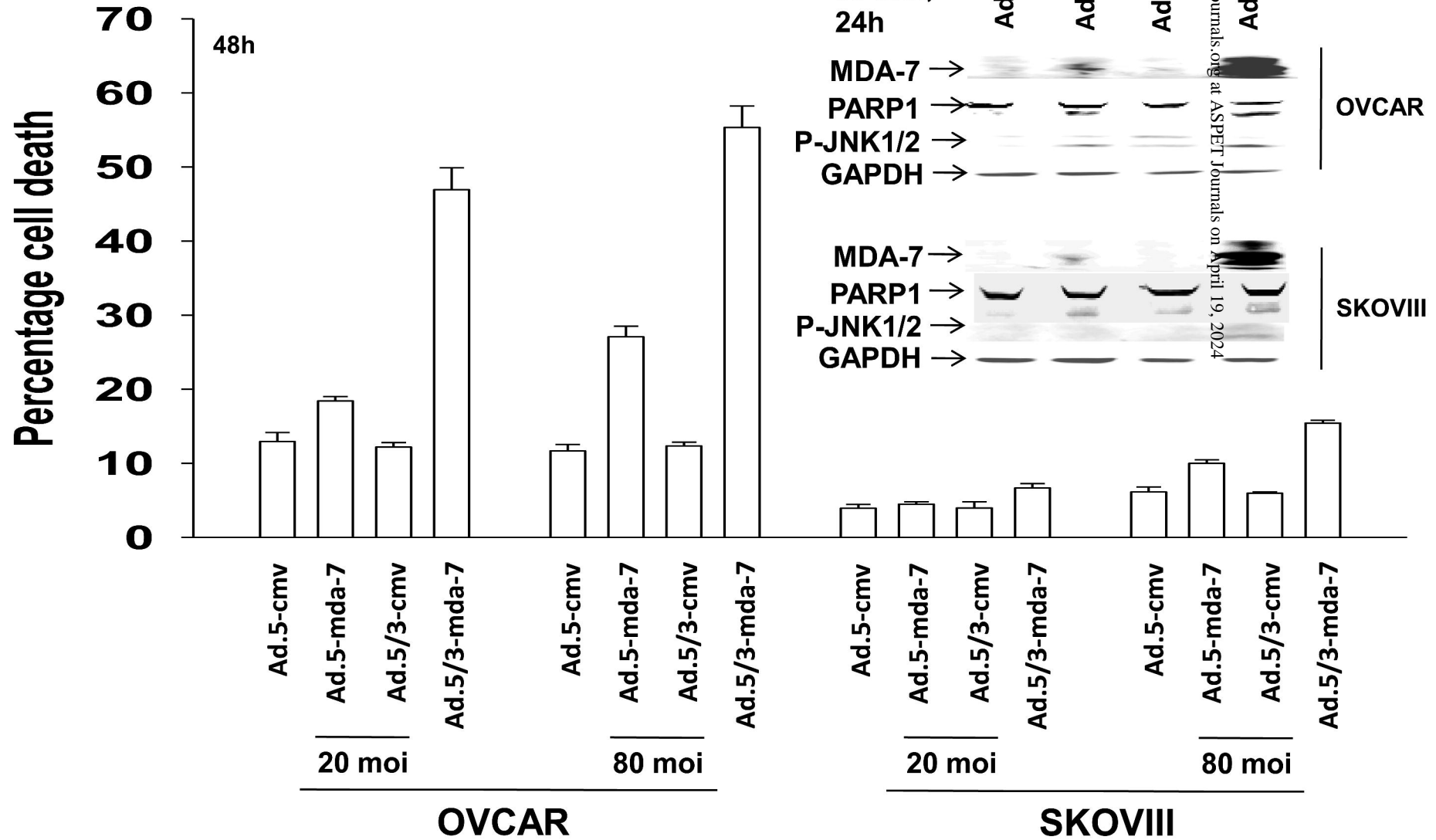


Figure 3B

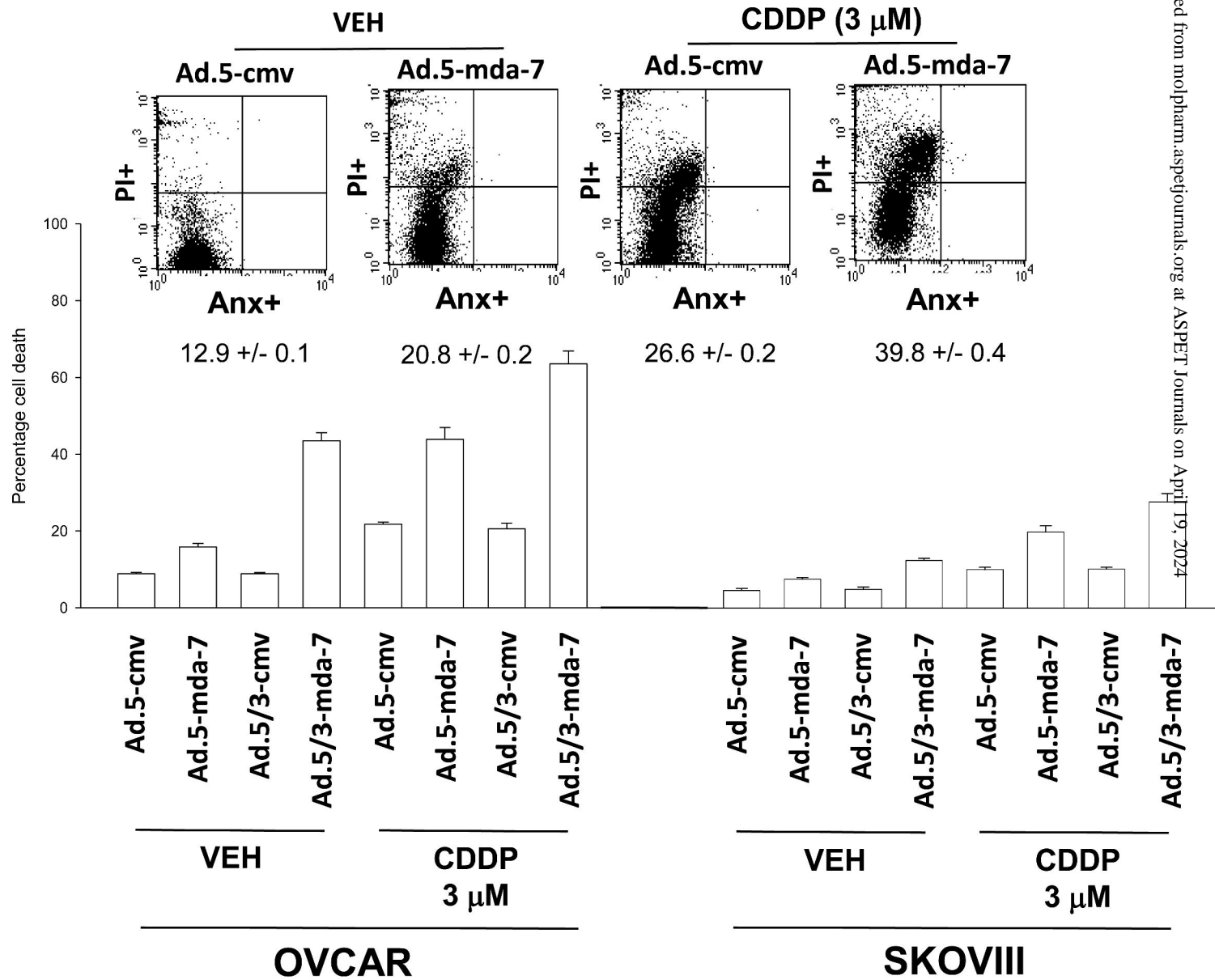


Figure 3C

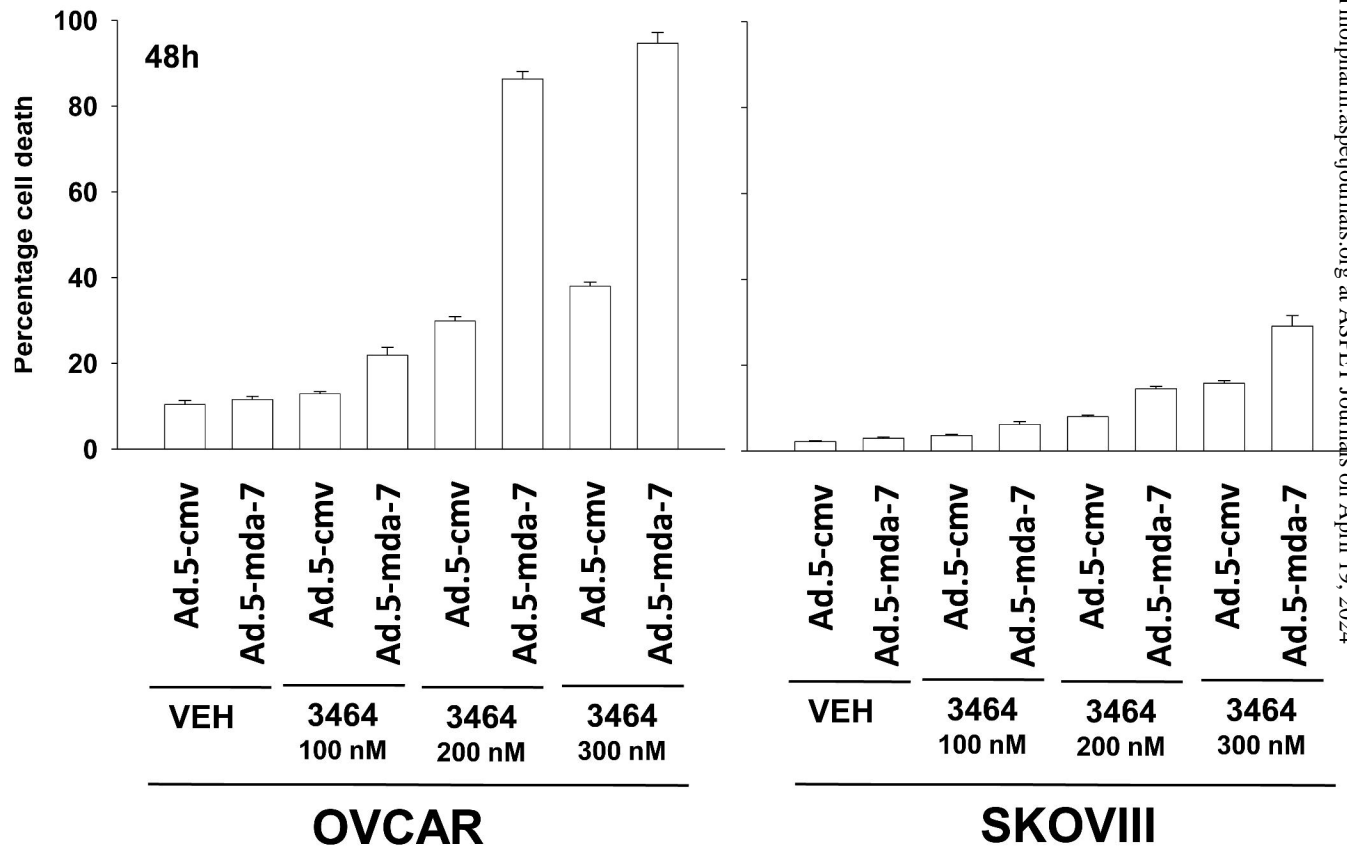


Figure 3D

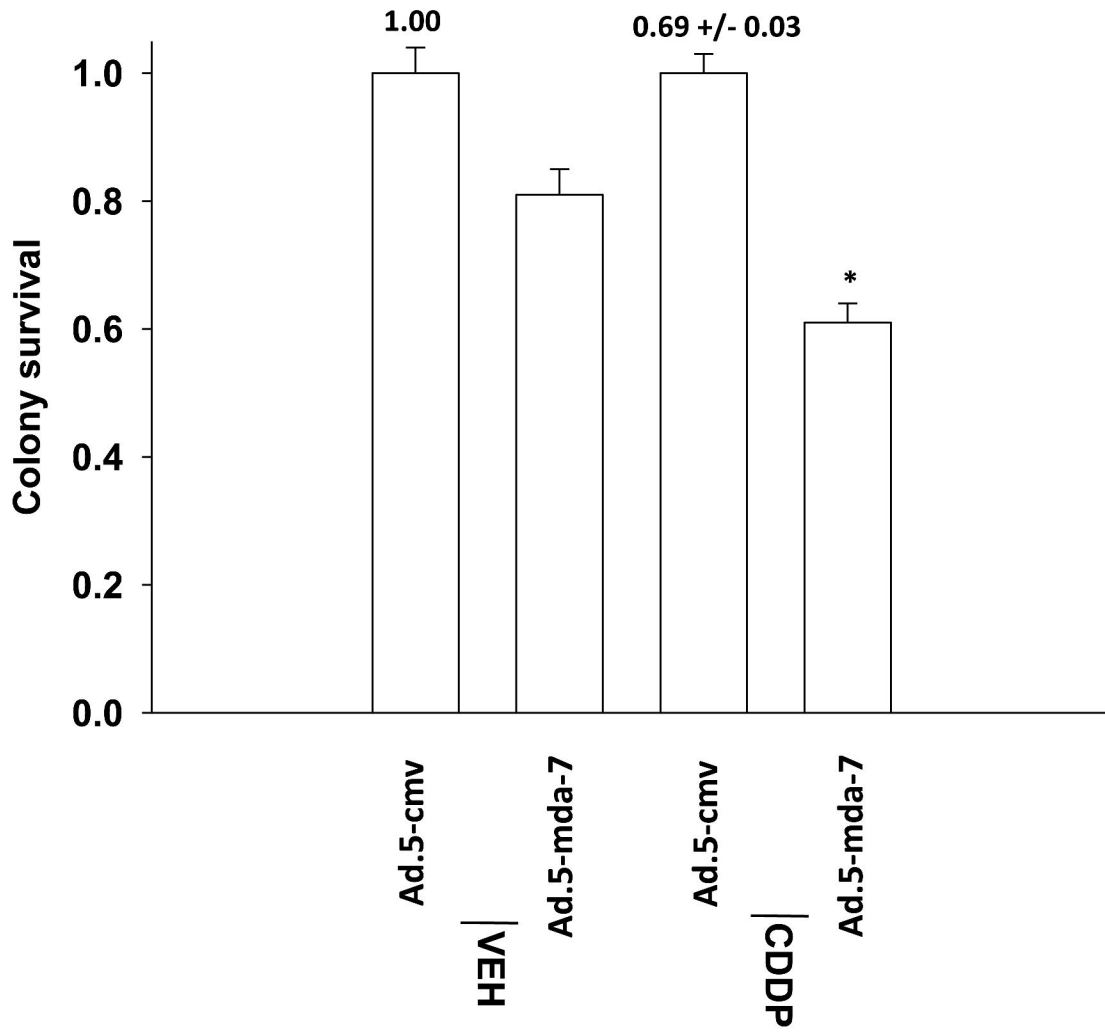
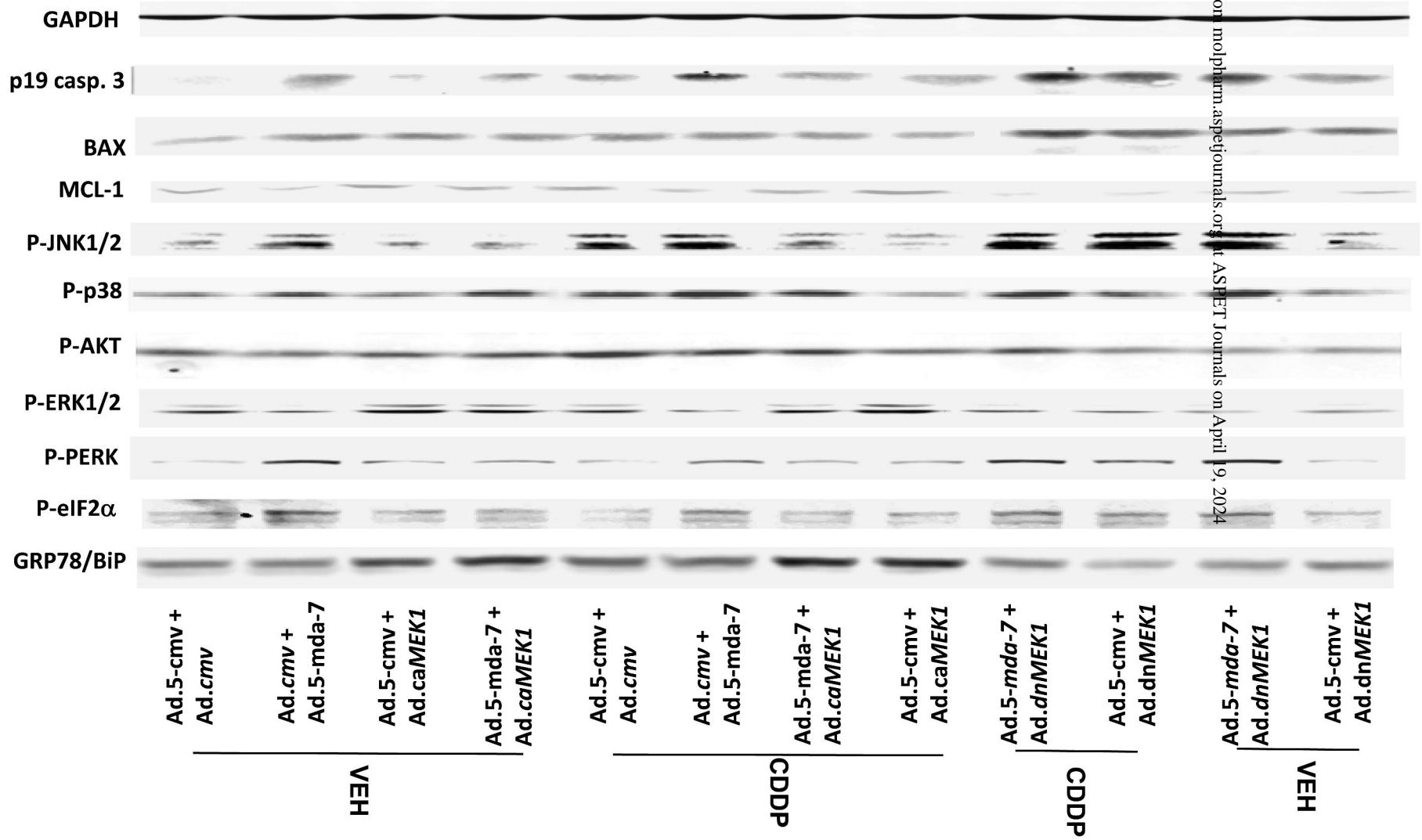


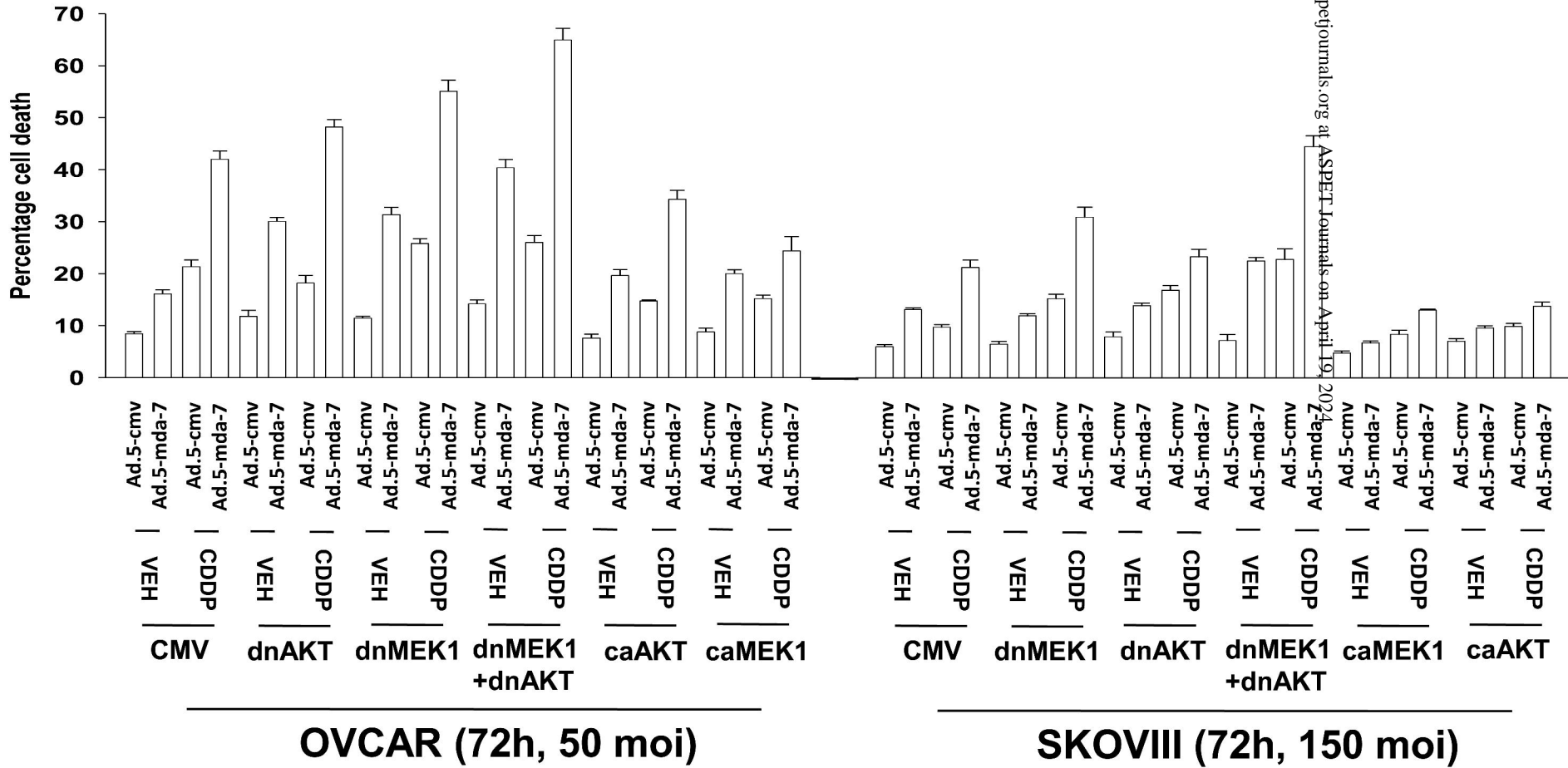
Figure 4A

OVCAR



Downloaded from molpharm.aspetjournals.org at ASHET Journals on April 19, 2024

Figure 4B



Downloaded from molpharm.aspetjournals.org at ASPET Journals on April 19, 2024

Figure 4C

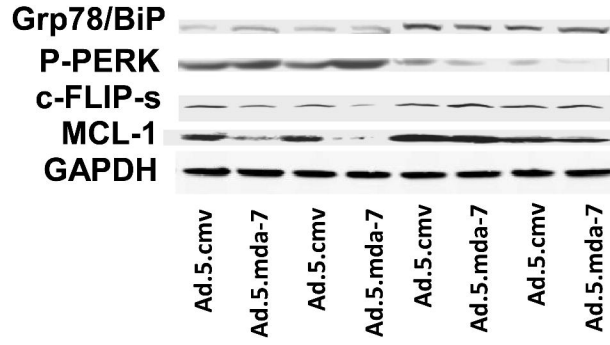
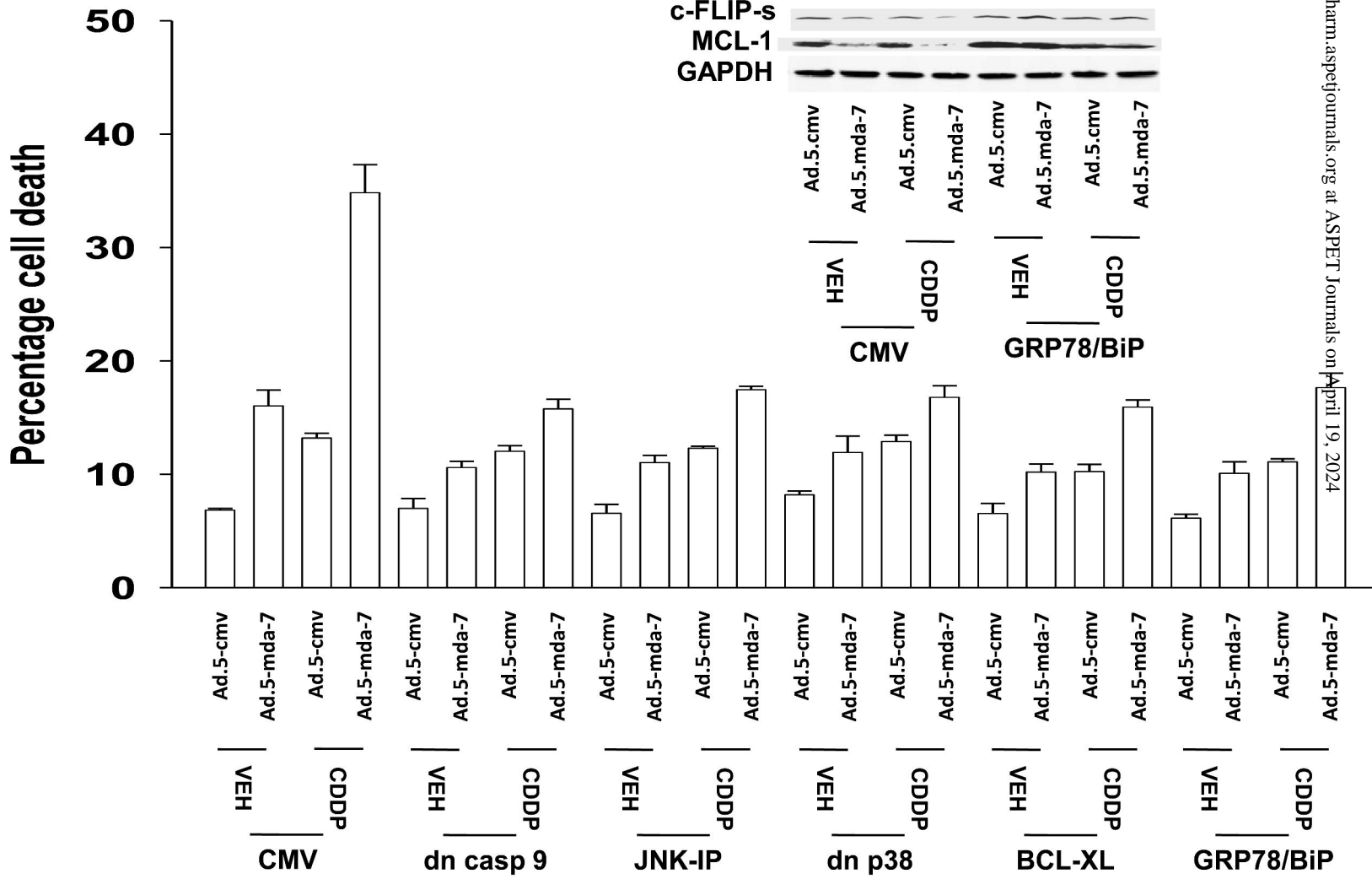


Figure 4D

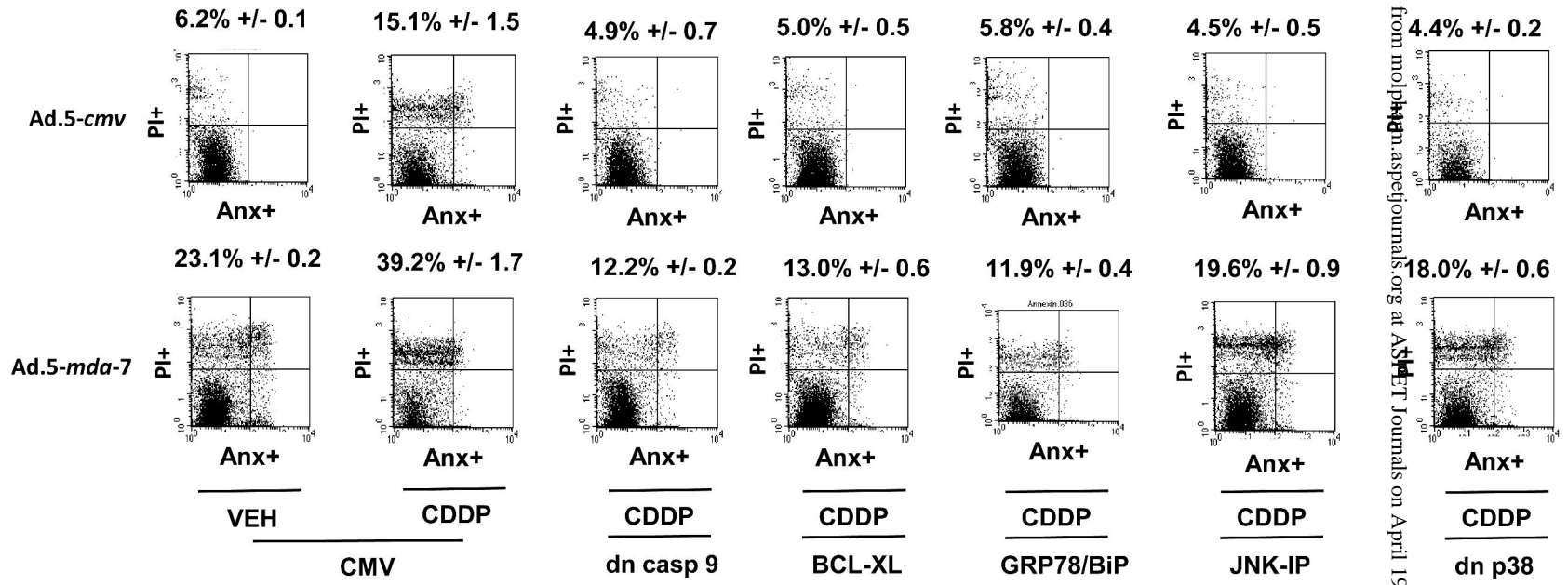


Figure 4E

Percentage cell death above vehicle control

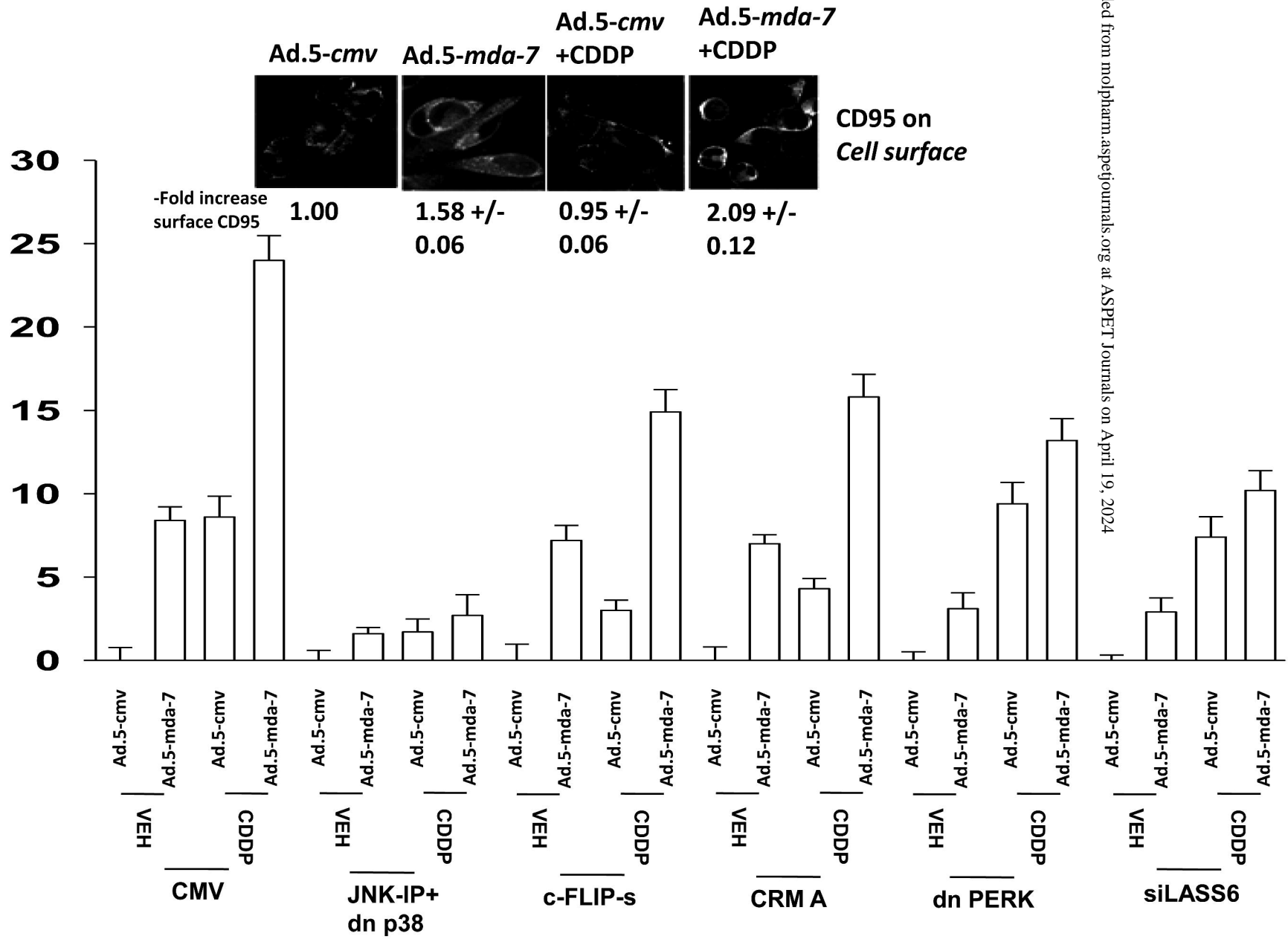
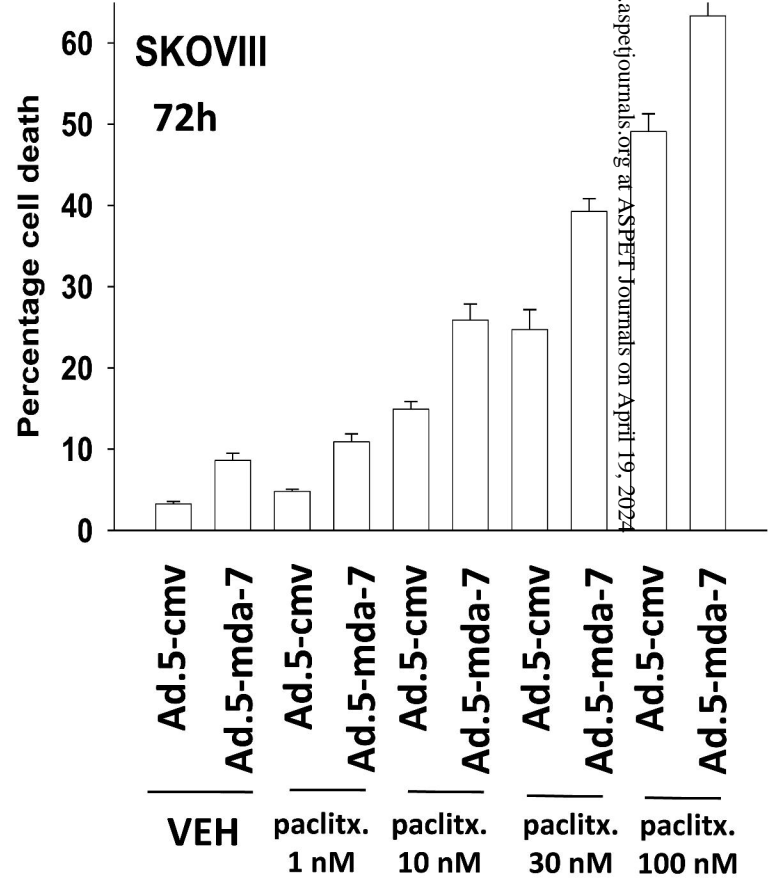
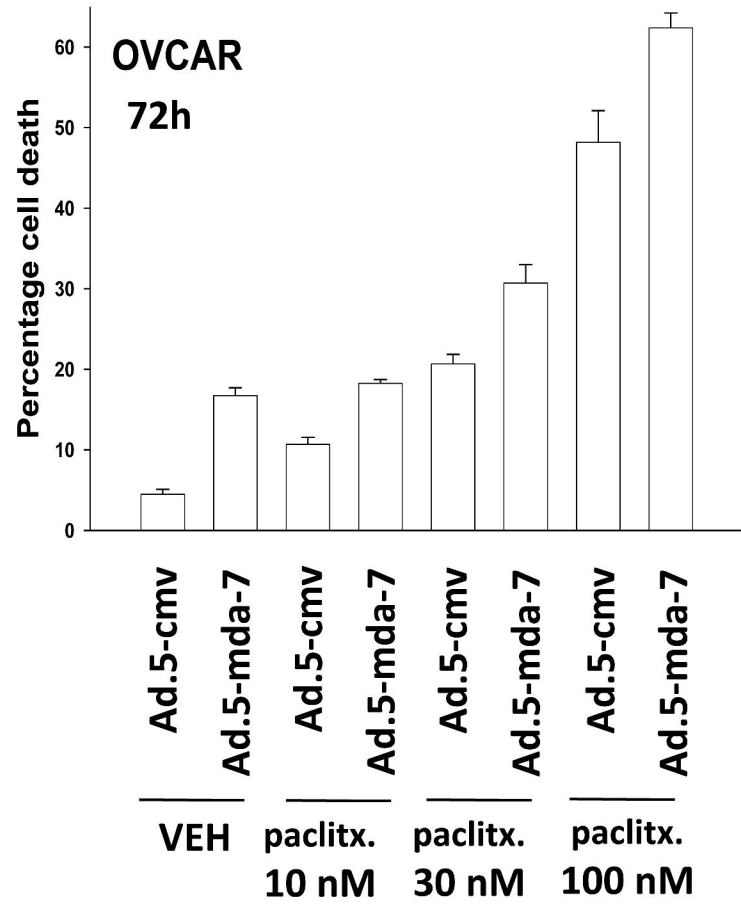


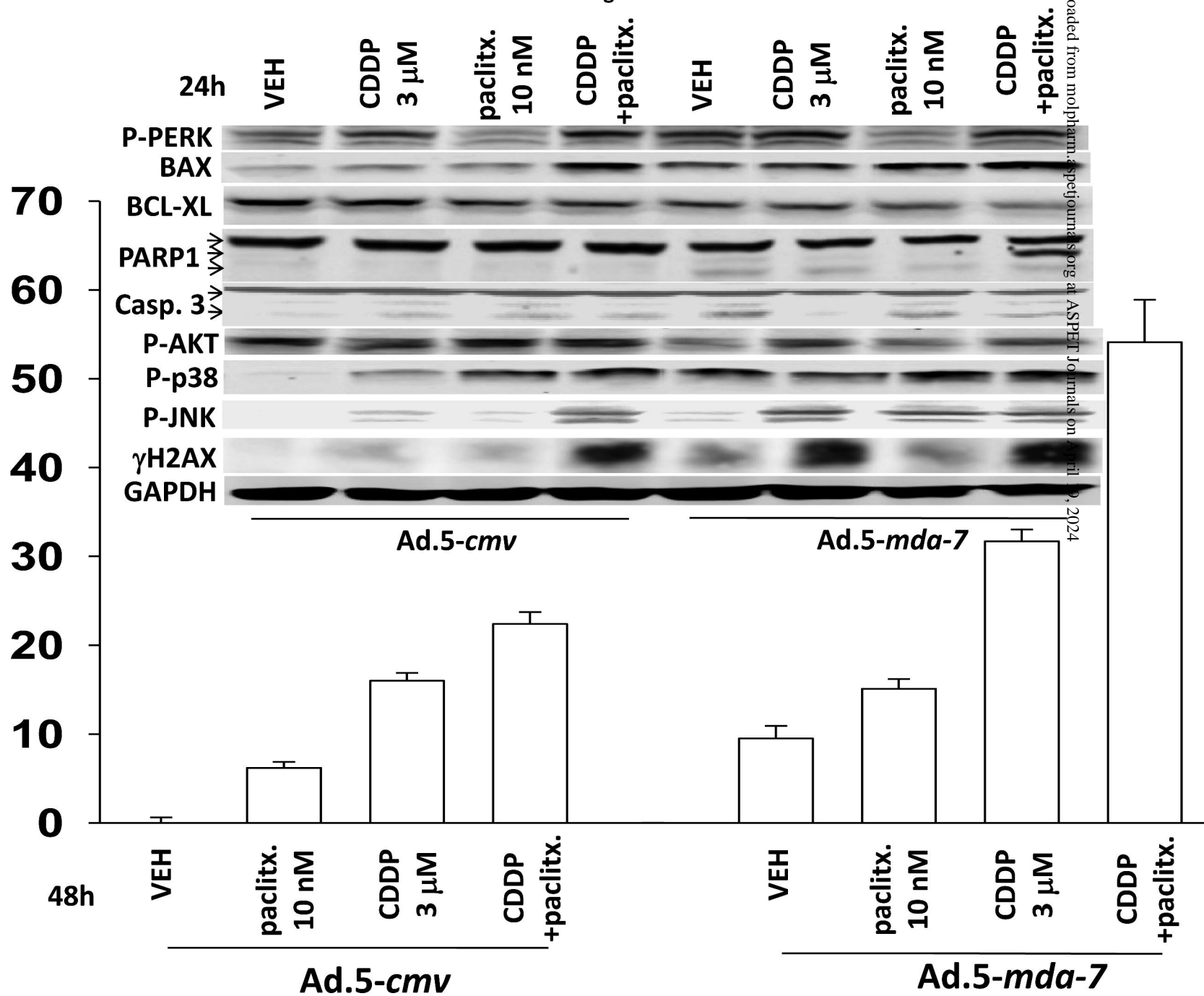
Figure 5A



Downloaded from molpharm.aspetjournals.org at ASPET Journals on April 19, 2024

Figure 5B

Percentage cell death above vehicle



Downloaded from molpharm.aspetjournals.org at ASPET Journals on April 10, 2024

Figure 5C

